IEEE Access
Multidisciplinary | Rapid Review | Open Access Journal

Received April 25, 2020, accepted May 1, 2020, date of publication May 4, 2020, date of current version May 20, 2020.

Digital Object Identifier 10.1109/ACCESS.2020.2992281

Analysis of Oscillatory Behavior of Heart by Using a Novel Neuroevolutionary Approach

ADNAN KHAN[1], MUHAMMAD SULAIMAN[1], HOSAM ALHAKAMI[2,3], AND AHMAD ALHINDI[2,3], (Member, IEEE)

[1]Department of Mathematics, Abdul Wali Khan University, Mardan 23200, Pakistan
[2]Department of Computer Science, Umm Al-Qura University, Mecca 21955, Saudi Arabia
[3]Center of Innovation and Development in AI (CIADA), Umm Al-Qura University, Mecca 21955, Saudi Arabia

Corresponding author: Muhammad Sulaiman (msulaiman@awkum.edu.pk)

The authors would like to thank the Deanship of Scientific Research at Umm Al-Qura University for supporting this work by Grant Code: 19-COM-1-01-0022.

ABSTRACT This paper aims at the analysis of the VdP heartbeat mathematical model. We have analysed the conditionality of a mathematical model which represents the oscillatory behaviour of the heart. A novel neuroevolutionary approach is chosen to analyse the mathematical model. The characteristics of the cardiac pulse of the heart are examined by considering two major scenarios with sixteen different cases. Artificial neural networks (ANNs) are constructed to obtain the best solutions for the heartbeat model. Unknown weights are finely tuned by a combination of a global search technique the Harris Hawks Optimizer (HHO) and a local search technique the Interior Point Algorithm (IPA). Stable behaviour of solutions obtained by considering different cases demonstrates that the model under consideration is well-conditioned. The accuracy of our novel procedure is established by getting the lowest residual errors in our solution for all cases. Graphical and statistical analysis are added to further elaborate the accuracy of our approach.

INDEX TERMS Cardiac pulse model, hybridized soft computing, artificial neural networks, non-linear ordinary differential equations, heuristics, interior-point algorithm, Harris Hawks optimizer.

I. INTRODUCTION

The main objective of this work is to examine the efficiency of a novel neuroevolutionary approach consisting of hybridized heuristics. Our stochastic procedure is used to analyse the dynamics of nonlinear Van der Pol (VdP) based heartbeat mathematical model of second-order nonlinear ordinary differential equations (ODEs). The VdP oscillatory system has been used for the accurate, and theoretical insight to understand different behaviours of cardiac pulses [1]–[3], such as periodicity, erratic behavior, relaxation, and bifurcations [4]. In terms of nonlinear oscillator [5], [6], the modified form of VdP heart dynamic model is mathematically represented as following:

$$\ddot{x} + \alpha(x - v_2)(x - v_1)\dot{x} + \frac{x(x+e)(x+d)}{ed} = F(t), \quad x(0) = c_1 \quad and \quad \dot{x}(0) = c_2, \qquad (1)$$

in equation (1) the fiber of heart is represented by x, α is pulse shape modification factor of heartbeat. When the heart model is simulated, the value of α changes, parameters v_1 and v_2 which are asymmetric component that modify damping term that exist in typical VdP ordinary differential equation, e is the duration of ventricular contraction while the term d is a factor that is created to replace the harmonic force term in standard VdP equation with the cubic term and the factor $F(t)$ on right hand side of equation (1) is representing the external force factor. System in equation (1) is a nonlinear, second-order differential equation with two initial conditions representing a well-posed problem. Exact solution for VdP nonlinear oscillatory system is not available. Due to this reason, various numerical and exact methods are designed to find out the approximate solutions. For example, the Adomian Decomposition Method (ADM) [7], [8], He's parameter expanding method [9], Laplace Decomposition Method (LDM) [10], method of linearization [11] and Homotopy Analysis Method (HAM) [12], etc. All these methods have their own applications, characteristics and limitations, but the stochastic techniques has its own organized potency, because of their strength. Moreover, techniques listed above are rarely used for the solution of Van der Pol dynamic model in the field of bio-informatics.

The associate editor coordinating the review of this manuscript and approving it for publication was Ali Salehzadeh-Yazdi.

Artificial intelligence techniques are considered effective, accurate and reliable for the solution of many unconstrained and constrained optimization problems arising in different fields [13]–[15]. Some recent artificial intelligence methodologies based on artificial neural networks (ANNs) appeared with different applications [16], [17]. These include second-kind fredholm integral equations [18], analysis the bending of beam column [19], astrophysics models [20], bilinear programming problems [21] and inverse kinematic problems [22].

Feed-forward ANNs are used as universal function approximation procedures for the development of stochastic numerical solvers. Due to their strength and stability, they are widely used for the solutions of nonlinear systems [23]–[27]. By combining global search and local search optimization approaches, these networks are typically optimized by reducing the residual errors in solutions. Recent implementation of these methods is the solution of VdP oscillatory nonlinear systems [28], [29], fractional optimal control problems [30], [31], fuel ignition model in the theory of combustion, longitudinal heat transformation fins model [32], nano-fluidics problems, the fuel ignition mechanism in the theory of combustion [33], Navier Stoke's equations [34], the longitudinal heat transfer fins model [35], [36], nonlinear Troesch form equations in the field of plasma physics [37], [38], thin film flow problems in fluid mechanics [39], system of linear Volterra integral equations [40], pantograph form of functional ODE and boundary value problems (BVPs) [41], [42], traveling singularity problems of the nonlinear Painleve form equations [43], magneto-hydro dynamics (MHD) study [44]–[46], electrical conducting solids models [47], electromagnetic theory problems [48], fuzzy differential equations [49], [50], the study of spherical cloud model in thermodynamics [51], nonlinear equations of Lane Emden form [51]–[53] and nonlinear systems of fractional order [54], [55].

These methodologies have encouraged many researchers to scrutinize explicitly the stability and power of stochastic numerical techniques to build an alternative, yet simple, precise, intelligent, efficient, stable, steady computing systems to examine the problems like VdP model of the heartbeat.

In this research article, a stochastic technique is established based on feed-forward ANNs which are optimized with a hybrid of the "Harris Hawks Optimizer" (HHO) and the "Interior Point Algorithm" (IPA). This soft computing paradigm is used to analyse the VdP nonlinear dynamic heartbeat model as in equation(1). Global and local search characteristics of HHO and IPA are combined to optimize the design parameters of the ANNs for solutions of VdP nonlinear dynamic heartbeat model. The results of the proposed method for the model (1) are compared with reference numerical solutions to verify the accuracy of the proposed method. Four main scenarios and sixteen different cases are considered by varying the factor of external forcing, damping coefficients, and pulse shape modification factor, while the value of the ventricular contraction period is kept constant.

The convergence and accuracy of our results obtained by the proposed scheme are statistically analysed in terms of standard deviation, mean square errors, absolute errors, mean absolute deviation (MAD), root-mean-square error (RMSE), and error in Nash–Sutcliffe efficiency (ENSE) by using results of multiple independent runs. Moreover, Nash Sutcliffe efficiency illustrates its reliability, applicability, and effectiveness.

II. HEART BEAT MODELING BASED ON VAN DER POL NONLINEAR OSCILLATOR

In this portion of the paper, we describe the essential background of the Van der Pol (VdP) model as presented in equation (1). The Van der Pol oscillators which are also known as relaxation oscillators, were originally proposed for modelling of electronic circuits [56] in electrical engineering and are been frequently used in theoretical models of biological sciences like cardiac rhythm. The following nonlinear oscillatory model [56], [57] is a system based mathematical modeling of VdP heart model:

$$\ddot{x} + \alpha(x^2 - 1)\dot{x} + \omega x = 0, \tag{2}$$

here ω and α in system (2) are constant coefficients, associated to duffing and damping parameters of the system.

In the terms of synchronization, chaos and limited cycles, VdP equation is similar to biological systems and that is why VdP system based differential equations are frequently used in representations of theoretical heart oscillations [1], [2], [4], [5], [7], [9], [12]. Moreover, VdP equation generates the external dynamic frequency of pacemaker, without any variation in amplitude and this is a vital particularity of the cardiac pacemaker. Zebrowski and Grudzinski were first to introduce these classical VdP models of heart [1].

Later on scientists modified the classical model of VdP and the properties of VdP model of heart are dramatically changed by fixing stable and saddle locations as $x = -2d$ and $x = -d$ respectively. Voltage related VdP heart model with updated terms of asymmetric damping is as follows:

$$\ddot{x} + \alpha(x^2 - \mu)\dot{x} + \frac{x(x+d)(x+2d)}{d^2} = 0. \tag{3}$$

The distance among these fixed points can not be changed, so for further modification in equation (3) and changes in depolarization period another parameter e is introduced as follows:

$$\ddot{x} + \alpha(x^2 - \mu)\dot{x} + \frac{x(x+e)(x+d)}{ed} = 0, \tag{4}$$

the damping term $\alpha(x^2 - \mu)$ is replaced with $(x - v_2)(x - v_1)$, which is asymmetric with respect to the variable x, for further updates in (4) it is modified as [4], [29], [56], [58]:

$$\ddot{x} + \alpha(x - v_2)(x - v_1)\dot{x} + \frac{x(x+e)(x+d)}{ed} = 0. \tag{5}$$

The conditions $v_1, v_2 < 0$, must be satisfied to keep up the automatic oscillatory feature of heart. The modified model has the capability mathematically represent the fundamental physical characteristics of heart pulse subject to normal conditions. But in the presence of external forcing factor or external pacemaker $F(t)$, system in equation (5) is given as:

$$\ddot{x} + \alpha(x - v_2)(x - v_1)\dot{x} + \frac{x(x+e)(x+d)}{ed} = F(t), \quad x(0) = c_1, \quad \text{and} \quad \dot{x}(0) = c_2. \tag{6}$$

The given system in equation (6) is a nonlinear VdP oscillations based heart model to examine the characteristics of a cardiac pulse. Extra information about the given model is in [59].

III. PROPOSED DESIGN OF SOFT COMPUTING

The proposed soft computing scheme for the study of heart dynamics model, consists of two parts, in the very first part of the scheme an unsupervised ANNs model is designed for the system of a differential equation (1) and in the second part of the scheme unknown weights are finely tuned using a hybrid algorithm of the "Harris Hawks Optimizer" (HHO) and the "Interior Point Algorithm" (IPA). The designed methodology is graphically presented in figure (5).

A. SERIES SOLUTIONS FOR HEART BEAT MATHEMATICAL MODEL

The mathematical model for solutions of ordinary differential equations is formulated in the form of continuous mapping by manipulating the strength of approximation theory [58]. These networks and their n^{th}-derivatives of the solutions $x(t)$ are given as follow:

$$\begin{aligned}
\hat{x}(t) &= \sum_{j=1}^{m} \varphi_j f(w_j t + \beta_j), \\
\dot{\hat{x}}(t) &= \sum_{j=1}^{m} \varphi_j \dot{f}(w_j t + \beta_j), \\
\ddot{\hat{x}}(t) &= \sum_{j=1}^{m} \varphi_j \ddot{f}(w_j t + \beta_j), \\
&\cdots \quad \cdots \quad \cdots \\
&\cdots \quad \cdots \quad \cdots \\
&\cdots \quad \cdots \quad \cdots \\
\hat{x}^{(n)}(t) &= \sum_{j=1}^{m} \varphi_j f^{(n)}(w_j t + \beta_j),
\end{aligned} \tag{7}$$

in above equation (7), $\varphi = [\varphi_1, \varphi_2, \varphi_3, \ldots, \varphi_m]$, $w = [w_1, w_2, w_3, \ldots w_m]$ and $\beta = [\beta_1, \beta_2, \beta_3, \ldots, \beta_m]$ are real valued vectors with bounded ranges. Networks in (7) are activated with log-sigmoid function $\zeta(t) = 1/(1 + e^{-t})$ and the derivatives of log-sigmoid function in updated form are given in equations (8) below:

$$\begin{aligned}
\hat{x}(t) &= \sum_{j=1}^{m} \varphi_j \left(\frac{1}{1 + e^{-(w_j(t)+\beta_j)}} \right), \\
\dot{\hat{x}}(t) &= \sum_{j=1}^{m} \varphi_j w_j \left(\frac{e^{-(w_j(t)+\beta_j)}}{(1 + e^{-(w_j(t)+\beta_j)})^2} \right), \\
\ddot{\hat{x}}(t) &= \sum_{j=1}^{m} \varphi_j w_j^2 \left(\frac{2e^{-2(w_j t+\beta_j)}}{(1 + e^{-(w_j t+\beta_j)})^3} - \frac{e^{-(w_j t+\beta_j)}}{(1 + e^{-(w_j t+\beta_j)})^2} \right).
\end{aligned} \tag{8}$$

The mathematical model of (1) can be construct by using appropriate combination of neural networks given in equations (7) or (8). The graphical composition of neural network based solutions of VdP based heart model are presented in the form of input, hidden layers and output as given in figure (1).

1) FITNESS FUNCTIONS

Fitness function for finding best solutions to heart dynamics model (1) are constructed as optimization problems. A minimization objective function of mean squared error is formulated as:

$$minimize\ \varepsilon = \varepsilon_1 + \varepsilon_2, \tag{9}$$

where ε_1 denotes mean square error of the function in nonlinear VdP equation (5), which is formulated as:

$$\begin{aligned}
\varepsilon_1 = \frac{1}{N} \sum_{m=1}^{M} \Bigg(& \ddot{\hat{x}} + \alpha(\hat{x}_m - v_2)(\hat{x}_m - v_1)\hat{x}_m \\
& + \frac{\hat{x}_m(\hat{x}_m + e)(\hat{x}_m + d)}{e \times d} \Bigg)^2, \\
for\ N = \frac{1}{h}, \quad & \hat{x}_m = \hat{x}(t_m) \quad and \quad t_m = mh,
\end{aligned} \tag{10}$$

on the other hand ε_2 represents mean squared error related to given initial conditions as following:

$$\frac{1}{2}((c_1 + \hat{x}_0)^2 + (-\hat{c_2} + \dot{x}_0)^2). \tag{11}$$

With the help of a hybrid optimization technique we will tune the solution weights $w = [\varphi, w, \beta]$ for ANNs model, such that, the fitness value ε of the system (1) minimize solution to zero. In this case solution of heart beat dynamic model (1) will be an ideal or near to exact solution. i.e. if $\varepsilon \longrightarrow 0$ then $\hat{x}(t) \longrightarrow x(t)$.

B. HYBRID OPTIMIZER HHO-IPA

The unknown parameters of the ANNs model are required to be trained for getting the best solutions of nonlinear VdP dynamic heart model (1). To accomplish this task, we have combined two optimization algorithms to get an intelligence computing technique. This hybrid technique is based on the Harris Hawks Optimizer (HHO) and the Interior point algorithm (IPA). HHO is considered a nimble, accurate, intelligent, potent, and reliable technique in the class

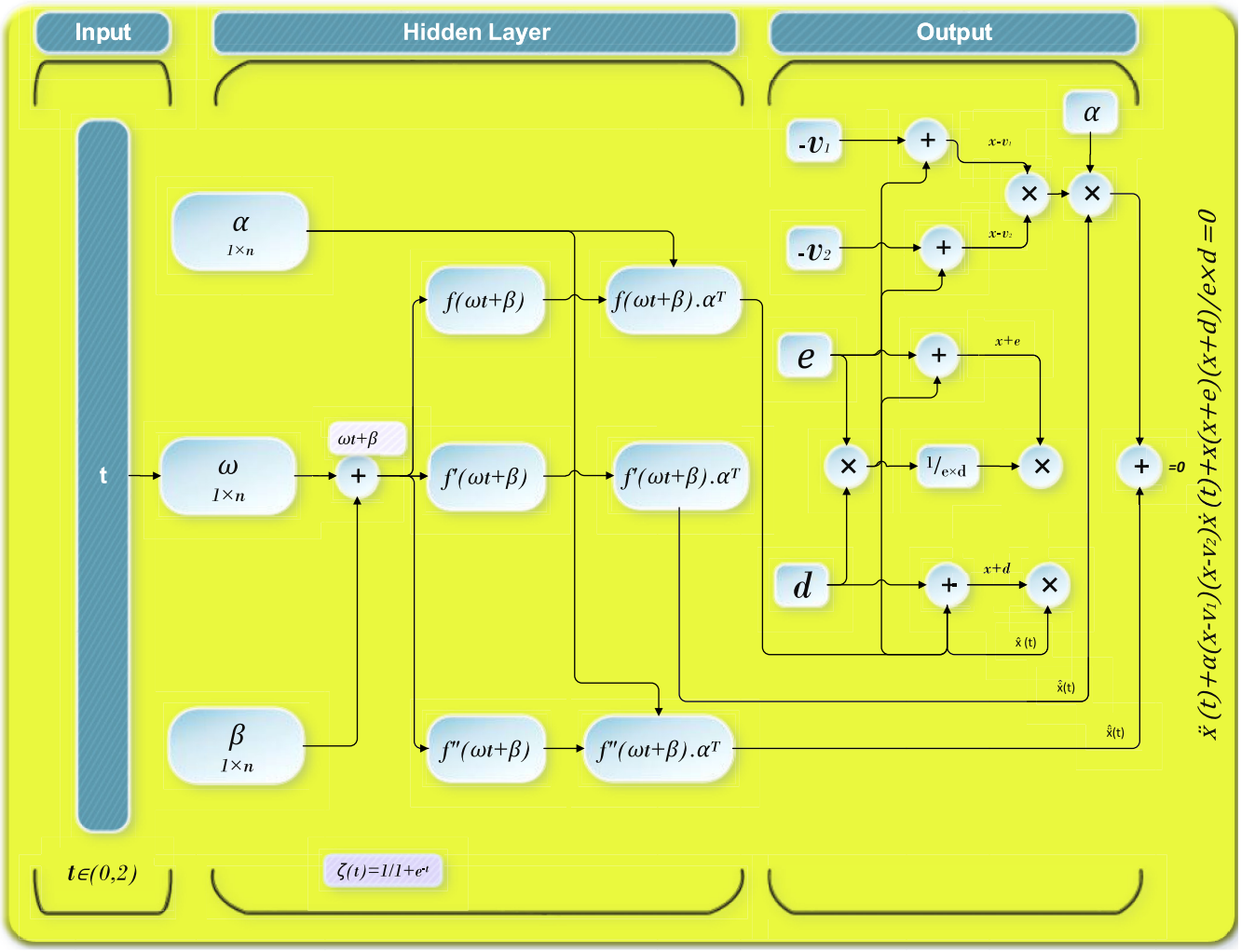

FIGURE 1. Graphical abstract of ANNs for Van der Pol dynamic heart model.

of particle swarm intelligence paradigms which are used mostly in various fields of numerical and applied sciences. This paradigm is Nature-inspired and was first introduced by Heidari *et al.* [60]. HHO is a global search technique, which means that it finds suitable or near best candidate solutions of the given optimization problems inside a unified search zone. The flowchart of HHO is in figure (2). HHO is an efficient optimizer to solve accurately unconstrained and constrained nonlinear optimization problems. The global search strength of HHO is hybridized with an effective local search algorithm, namely, IPA to get the best results rather quickly for an optimization problem. The finest individual solution of the global search algorithm HHO is selected as a starting point of local search technique IPA. Thus for quick and further tuning of unknown weights, IPA is used which is a single path following technique with better local search capability. The graphical abstract of IPA is given in figure (3) [61]. Many optimization problems are solved successfully by using IPA appearing in different fields, including hyperbolicity cone problems [62], nonlinear non-convex programming [63], parameter approximation of discrete-time infective disease models [64] and the flow of optimal power with FACTS devices [65], solutions of these problems motivated us to choose IPA, which is an interesting choice for local search.

Keeping in mind the power of HHO as a global search technique and IPA as a local search technique, a hybrid computing scheme HHO-IPA in figure (5) is applied for obtaining suitable design parameters of ANNs model to get solutions to the system of heartbeat model as shown in equation (1). For HHO we will use MATLAB script while IPA is executed in Matlab toolbox built-in function ''fmincon''. Proposed scheme HHO-IPA is sensitive to settings in tables (1) and (2), a small change in these settings may cause premature convergence of the algorithm. Parameters settings are prepared with comprehensive experimentations and care.

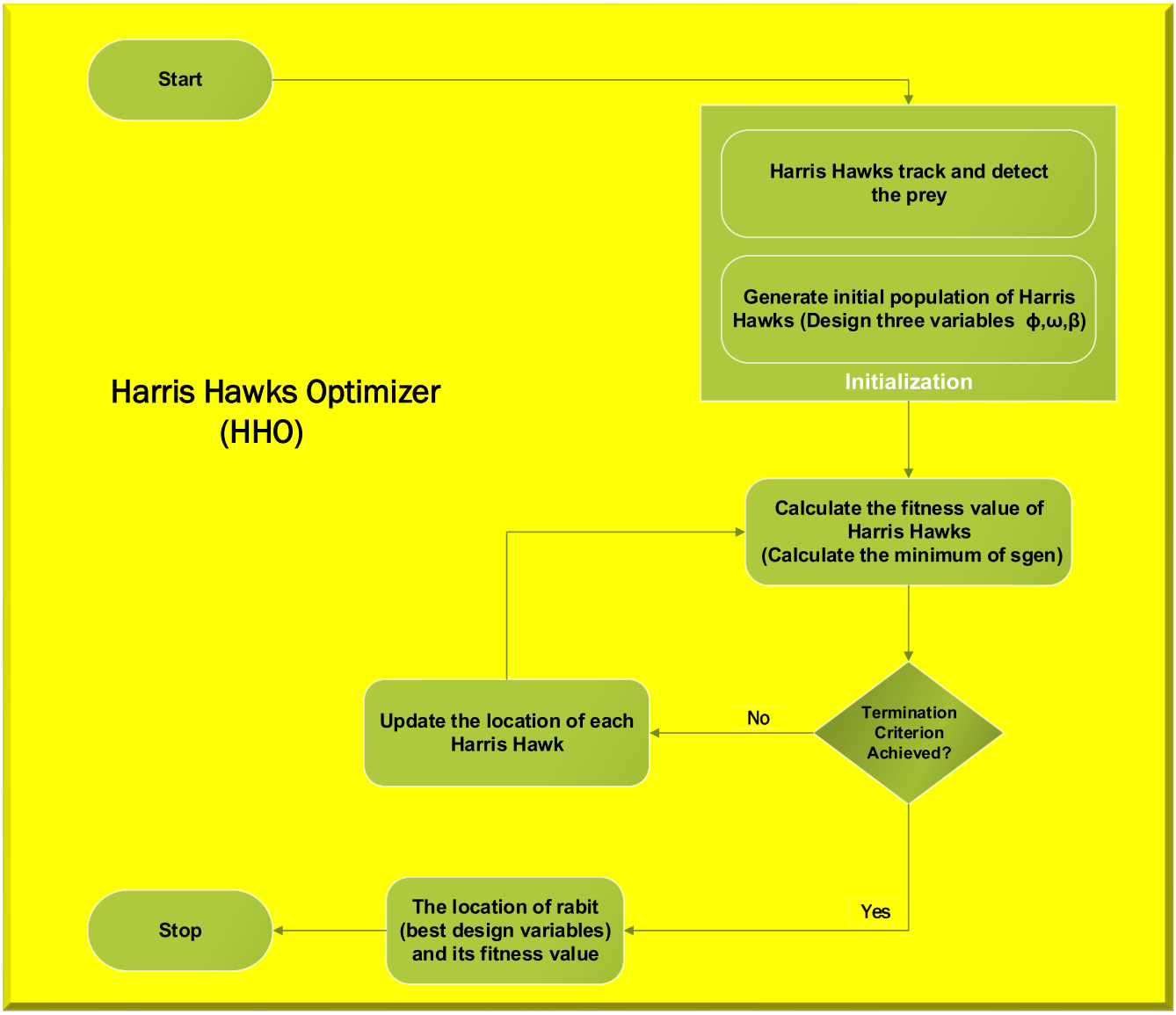

FIGURE 2. Flowchart of Harris Hawks Optimizer (HHO).

TABLE 1. Setting of parameters used for Harris Hawks Optimization.

Parameters	Settings	Parameters	Settings
Bounds [lower, upper]	[-30 30]	Maximum iterations	1000
Search agents	30	Population creation	Uniform

IV. EXPERIMENTAL SETUP AND RESULTS

In this section we present our results obtained by the hybrid soft computing approach for two major scenarios with sixteen different cases related to the VdP heartbeat model, see figure (4). The problem considered here is a generalized VdP equation with initial conditions. It consists of a second-order, nonlinear ordinary differential equation (ODEs) given as an initial value problem (IVP). Different cases are taken for each scenario based on different values of asymmetric damping terms, i.e. v_1 and v_2, and pulse shape modification factor α. The results of the proposed scheme are compared with the reference numerical solutions obtained from the Adams method (AM). The worth of the proposed scheme is proved through the numerical and graphical interpretation of the results.

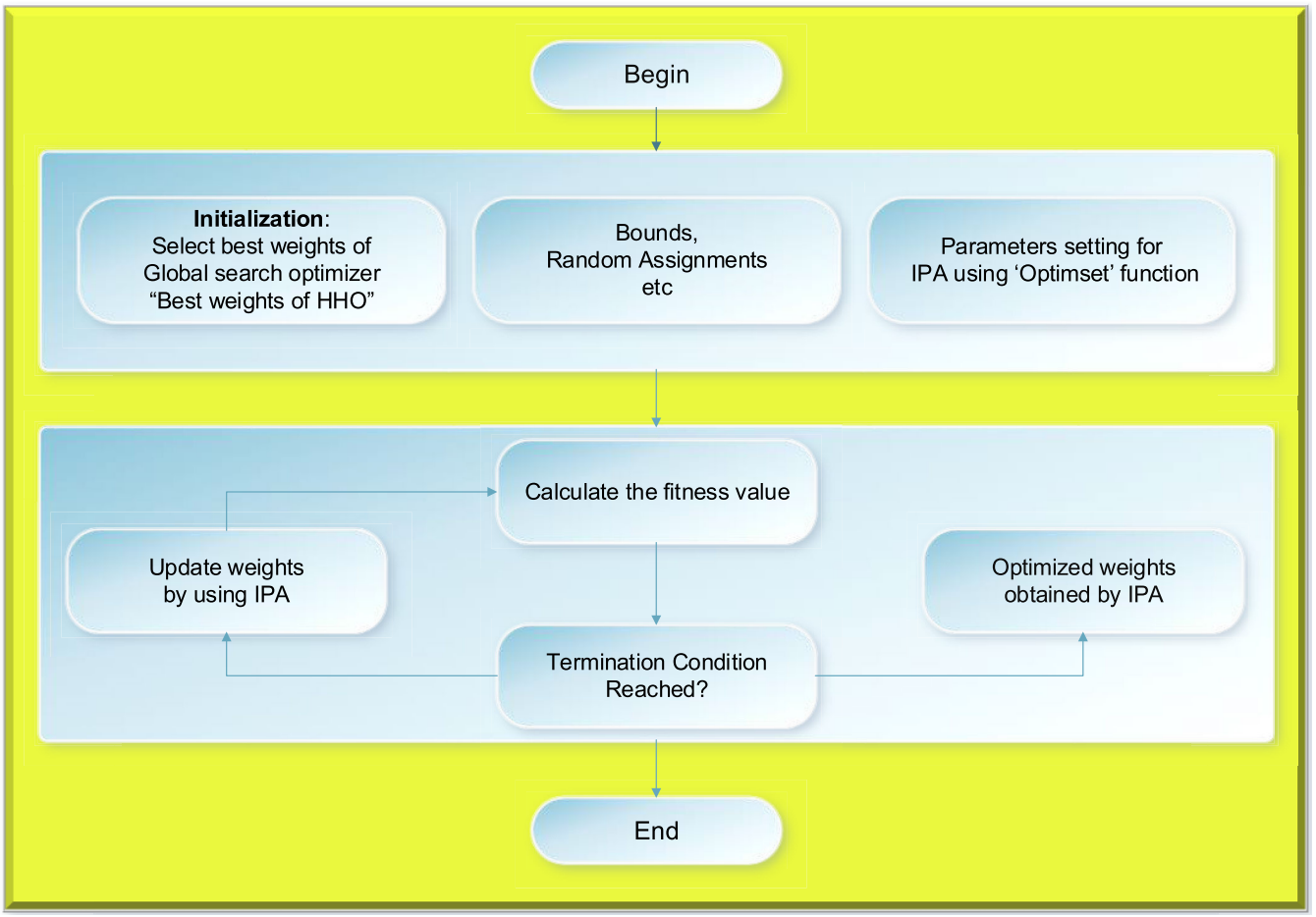

FIGURE 3. Illustration of the IPA.

TABLE 2. Setting of parameters used for "fmincon" program for the implementation of "interior point algorithm".

Parameters	Settings	Parameters	Settings
Upper bounds	$[10]_{1\times 30}$	Maximum iterations	5000
Lower bounds	$[-10]_{1\times 30}$	Hessian	BFGS
Scaling	Objective and Constraints	Max.function evaluations	$320,000$
Algorithm	'Interior-point algorithm'	X-Tolerance 'TolX'	10^{-22}
Relative tolerance	0.1	'TolCon'	10^{-18}
Initial weights	HHO global best	'TolFun'	10^{-18}
Type of finite difference	'Central'	Other	Default

A. PROBLEM-1: VDP DYNAMIC HEARTBEAT MODEL IN THE ABSENCE OF FORCING TERM

Two different scenarios are taken into this problem. Scenario-1 is taken based on changes in pulse shape modification term α while scenario-2 consider the changes in asymmetric damping terms (v_1, v_2) which represent terms associated to the voltage of heartbeat dynamic model (1), in the absence of forcing term $F(t)$ that appears in a normal state of a natural pacemaker. While d represents the coefficient of cubic factor which switches to harmonic forcing term and the term e in classical VdP equation is constant and is used to tune period of ventricular contraction [4], [29], [56], [58].

(a) Scenario-1: Effects of variations in pulse shape modification factor "(α)" of heartbeat model. To analyse the effects of changes in value of "(α)" we considered four cases as follows [58]:

Case$_1$: Consider Dynamic heartbeat model for $v_1 = 0.83$, $e = 6$, $d = 3$, $v_2 = -0.83$, and $\alpha = 3$.

Case$_2$: Consider Dynamic heartbeat model for $v_1 = 0.83$, $e = 6$, $d = 3$, $v_2 = -0.83$, and $\alpha = 2$.

Case$_3$: Consider Dynamic heartbeat model for $v_1 = 0.83$, $e = 6$, $d = 3$, $v_2 = -0.83$, and $\alpha = 1$.

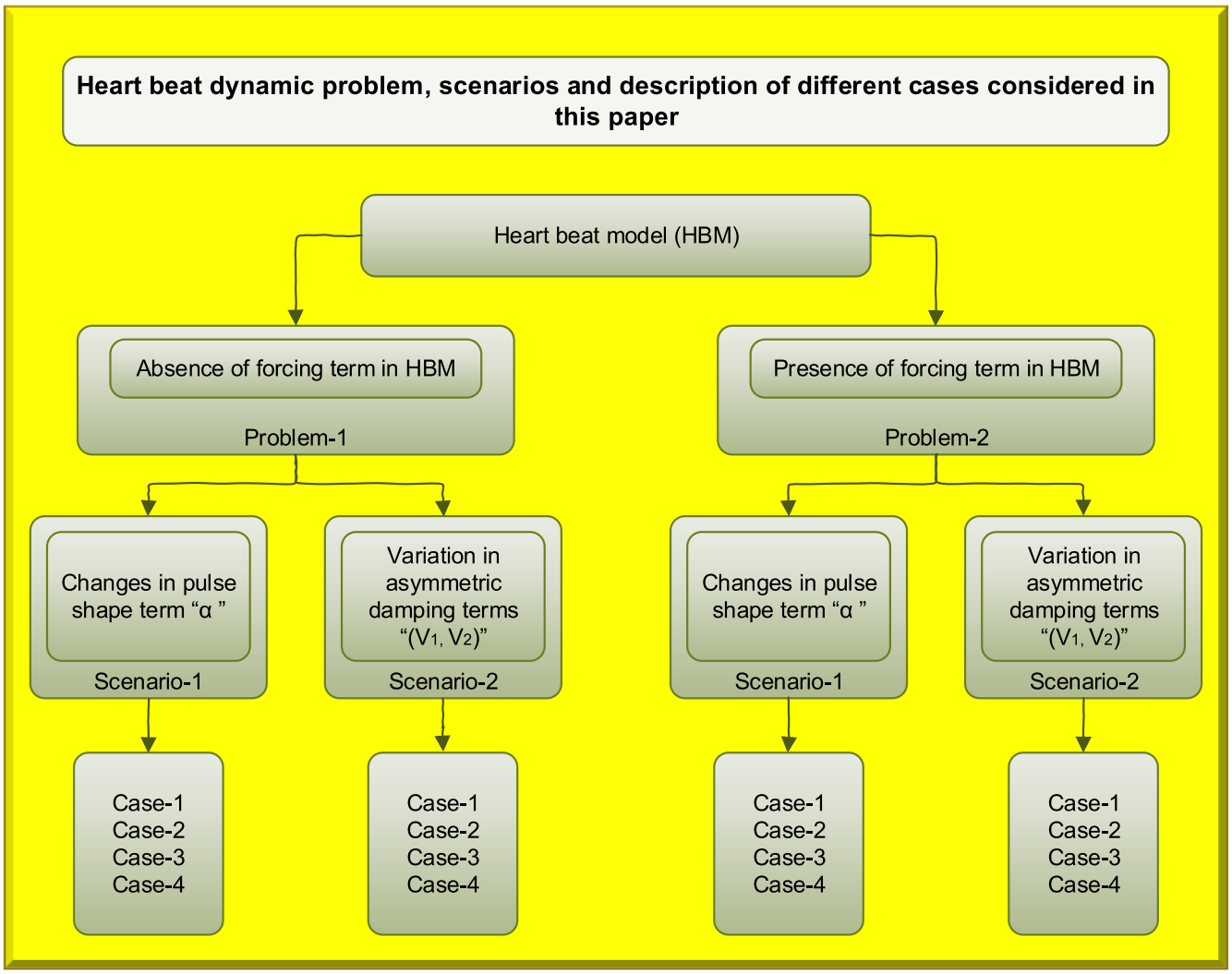

FIGURE 4. Graphical overview of problems 1, 2: Scenarios and cases considered in this paper for VdP dynamics heartbeat model.

Case$_4$: Consider Dynamic heartbeat model for $v_1 = 0.83$, $e = 6$, $d = 3$, $v_2 = -0.83$, and $\alpha = 0.01$.

The VdP nonlinear equation, obtained for the present scenario with corresponding initial conditions can be written as follows:

$$\ddot{x} + \alpha(x - 0.83)(x + 0.83)\dot{x} + \frac{x(x+6)(x+3)}{18} = 0, \quad x(0) = -0.1 \quad and \quad \dot{x}(0) = 0.025, \tag{12}$$

equation (12) represents the cases C_1, C_2, C_3 and C_4, for α equal to 3, 2, 1 and 0.01 accordingly.

Exact solution for the system in equation (12) does not exist, while the best numerical solutions of respective cases of the current scenario are determined with state-of-the-art "Runge Kutta Method" (RKM) using Matlab function *ode*45. The performance of designed scheme is compared with the reference solutions of RKM for solutions with inputs x in $[0, 2]$ and with a step size of $h = 0.1$. The proposed methodology described in the last section is used to solve (12), while the fitness function (FF) for this scenario is given as following:

$$\varepsilon = \frac{1}{N}\sum_{m=1}^{N}\left(\dot{\hat{x}}_m + \alpha(\hat{x}_m - 0.83)(\hat{x}_m + 0.83)\hat{x}_m + \frac{\hat{x}_m(\hat{x}_m+6)(\hat{x}_m+3)}{18}\right)^2 + \frac{1}{2}\left((\hat{x}_0 + 0.1)^2 + (\hat{x}_0 - 0.025)^2\right). \tag{13}$$

Optimization of the fitness function (FF) (13) is performed with the proposed hybrid scheme HHO-IPA and we got the best set of trained weights with fitness values for the cases C_1, C_2, C_3 and C_4 as 6.6486×10^{-12}, 1.0447×10^{-11}, 4.7537×10^{-13} and 2.0005×10^{-12} respectively, see figure (6). Solutions for the four cases, i.e. $\hat{x}_{c_1}$, $\hat{x}_{c_2}$, $\hat{x}_{c_3}$ and $\hat{x}_{c_4}$ are derived

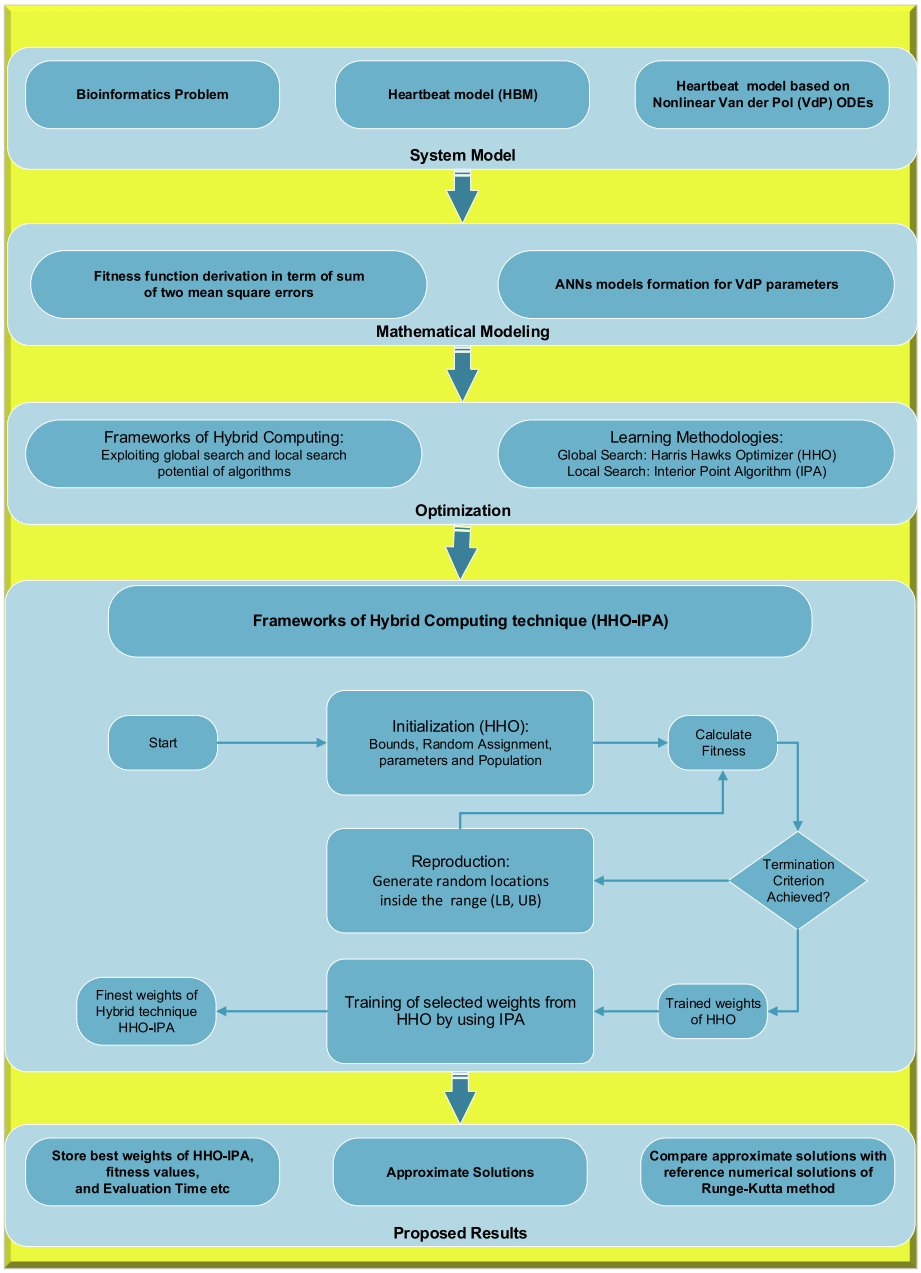

FIGURE 5. Graphical flowchart of designed technique for solution of VdP dynamics heartbeat model.

using the weights of figure (7) and are given as follows:

$$\hat{x}_{c_1} = \begin{Bmatrix} \frac{-2.1285}{1+e^{-(0.4053t-0.4084)}} + \frac{1.3586}{1+e^{-(-0.3502t-2.6372)}} \\ + \frac{-0.3400}{1+e^{-(2.5582t-3.196)}} + \frac{1.8950}{1+e^{(-0.6294t-1.4909)}} \\ + \frac{1.7623}{1+e^{-(0.7653t-0.3561)}} + \frac{-2.9351}{1+e^{-(1.5600t-3.2773)}} \\ + \frac{-0.1552}{1+e^{-(4.1185t-7.2004)}} + \frac{1.7523}{1+e^{-(2.2227t-3.1798)}} \\ + \frac{-0.6997}{1+e^{-(1.1985t+0.1017)}} + \frac{1.5691}{1+e^{-(3.4598t-6.4259)}}, \end{Bmatrix} \tag{14}$$

$$\hat{x}_{c_2} = \begin{Bmatrix} \frac{2.1116}{1+e^{-(1.4039t-2.6925)}} + \frac{1.7800}{1+e^{-(-0.4214t+1.1213)}} \\ + \frac{-1.4704}{1+e^{-(-2.0080t+4.7784)}} + \frac{1.2812}{1+e^{-(0.3376t+1.3421)}} \\ + \frac{2.9244}{1+e^{-(-0.0213t-2.0010)}} + \frac{2.9515}{1+e^{-(-0.7748t+2.1342)}} \\ + \frac{-2.4066}{1+e^{-(0.9261t-2.4286)}} + \frac{-2.6720}{1+e^{-(-0.1838t+0.6096)}} \\ + \frac{-2.6162}{1+e^{-(0.4300t+2.7706)}} + \frac{1.1361}{1+e^{-(1.3608t-1.1842)}}, \end{Bmatrix} \tag{15}$$

$$\hat{x}_{c3} = \begin{cases} \frac{2.0385}{1+e^{-(-0.8603t-0.9258)}} + \frac{2.8794}{1+e^{-(-0.7457t+1.3186)}} \\ + \frac{-0.5843}{1+e^{-(0.4312t-1.6624)}} + \frac{-2.9660}{1+e^{-(0.7879t-3.2565)}} \\ + \frac{-0.9673}{1+e^{-(-0.8462+1.3543)}} + \frac{-2.3247}{1+e^{-(-0.7660t-0.8856)}} \\ + \frac{2.0960}{1+e^{-(1.0508t-2.7546)}} + \frac{-0.9373}{1+e^{-(-0.8462t+1.3542)}} \\ + \frac{1.1136}{1+e^{-(-0.6014t-3.2555)}} + \frac{-0.9374}{1+e^{-(-0.8462t+1.3540)}}, \end{cases} \tag{16}$$

$$\hat{x}_{c4} = \begin{cases} \frac{0.3313}{1+e^{-(-0.3937t-0.1814)}} + \frac{1.7056}{1+e^{-(0.8318t-1.3627)}} \\ + \frac{0.7222}{1+e^{-(-0.3888t+0.5809)}} + \frac{-1.2072}{1+e^{-(-0.7245t-0.5976)}} \\ + \frac{0.4064}{1+e^{-(-1.0610t-1.2141)}} + \frac{-0.5178}{1+e^{-(0.2432t+0.5049)}} \\ + \frac{0.9205}{1+e^{-(-0.3752t-0.1277)}} + \frac{-0.9166}{1+e^{-(0.2678t+1.0637)}} \\ + \frac{0.0290}{1+e^{-(-1.3697t+2.0551)}} + \frac{-1.0858}{1+e^{-(0.4423t-1.6272)}}, \end{cases} \tag{17}$$

Solutions plotted in figure (6) are obtained by using inputs in interval $[0, 2]$ with the step size of $h = 0.1$ in equations (14-17), for heartbeat model (12), AEs are calculated for every case and are plotted in figure (6b). It is observed that the accuracy of order $10^{-13} - 10^{-11}$ is attained for the first two cases, however for the third case errors are much better as $10^{-12} - 10^{-15}$, and for last case the accuracy is even better by getting negligible errors as $10^{-12} - 10^{-14}$.

To find out the best weights for the ANNs model of the given equation (12) and to calculate the convergence and correctness of the proposed algorithm, 50 independent runs of the hybrid intelligent computation scheme HHO-IPA are performed. Statistical performance of HHO-IPA is shown based on the results which we have established after 50 independent runs. These statistical analyses are carried out in terms of the best solution, worst solution, mean values of absolute errors (AE) and standard deviation (STD), as given in table (3). It is clear that for these four cases i.e. C_1, C_2, C_3 and C_4 the mean error values are around $10^{-09} - 10^{-08}$, $10^{-08} - 10^{-06}$, $10^{-07} - 10^{-05}$ and $10^{-10} - 10^{-09}$. Furthermore, the minimum standard deviation for every case study of this scenario shows the coherent accuracy of our designed scheme.

(b) Scenario-2: Effects of variations in asymmetric damping terms (v_1, v_2) on the dynamic heartbeat model.

In this scenario we have studied the effects of variation in asymmetric damping parameters (v_1, v_2) on the heartbeat dynamic model. We have considered four cases for this purpose as follows:

Case$_1$: Consider Dynamic heartbeat model for $v_1 = 0.93$, $e = 6$, $d = 3$, $\alpha = 2$, and $v_2 = -0.93$.

Case$_2$: Consider Dynamic heartbeat model for $v_1 = 0.83$, $e = 6$, $d = 3$, $\alpha = 2$, and $v_2 = -0.83$.

Case$_3$: Consider Dynamic heartbeat model for $v_1 = 0.63$, $e = 6$, $d = 3$, $\alpha = 2$, and $v_2 = -0.63$.

Case$_4$: Consider Dynamic heartbeat model for $v_1 = 0.43$, $e = 6$, $d = 3$, $\alpha = 2$, and $v_2 = -0.43$.

The VdP nonlinear equation, obtained for the present scenario with corresponding initial conditions can be written as follow:

$$\begin{cases} \ddot{x} + 2(x - v_2(x - v_1))\dot{x} + \frac{x(x+6)(x+3)}{6 \times 3} = 0, \\ x(0) = -0.1 \quad and \quad \dot{x}(0) = 0.025, \end{cases} \tag{18}$$

equation (18) is analysed for four different cases C_1, C_2, C_3 and C_4 respectively for (v_1, v_2) chosen as $(0.93, -0.93)$, $(0.83, -0.83)$, $(0.63, -0.63)$ and $(0.43, -0.43)$.

Exact solution for the problem in equation (18) is also not known, for this reason, numerical solutions of equation (18) are calculated by using AM, and these solutions are used as reference points to calculate errors in our outcome. We have used the same experimental settings as in the previous scenario, but the fitness function is given as:

$$\varepsilon = \frac{1}{N}\sum_{m=1}^{N}\left(\hat{x}_m + 2(\hat{x}_m - v_2)(\hat{x}_m - v_1)\hat{x}_m + \frac{\hat{x}_m(\hat{x}_m+6)(\hat{x}_m+3)}{6\times 3}\right)^2 + \frac{1}{2}\left((\hat{x}_0 + 0.1)^2 + (\hat{x}_0 - 0.025)^2\right). \tag{19}$$

Weights for ANNs trained by HHO-IPA, with FF values for cases 1, 3 and 4, are 7.9429×10^{-12}, 2.3429×10^{-13} and 3.0588×10^{-13} respectively, and are graphically shown in figure (8). Corresponding solutions based on these weights are given as in 20-22:

$$\hat{x}_{c_1} = \begin{cases} \frac{-3.6967}{1+e^{-(-1.7278t+3.9495)}} + \frac{0.1434}{1+e^{-(-0.8181t-0.3241)}} \\ + \frac{0.0043}{1+e^{-(2.4621t-2.1053)}} + \frac{0.1373}{1+e^{-(-0.8423t-0.3244)}} \\ + \frac{4.1642}{1+e^{-(-1.8931t+4.9025)}} + \frac{0.0514}{1+e^{-(-0.6783t-0.3366)}} \\ + \frac{-1.2122}{1+e^{-(-2.7061t+5.9757)}} + \frac{1.1642}{1+e^{-(0.2985t-0.8385)}} \\ + \frac{-1.1322}{1+e^{-(-0.8168t-0.3253)}} + \frac{-0.1337}{1+e^{-(-0.8254t-0.3250)}}, \end{cases} \tag{20}$$

$$\hat{x}_{c_3} = \begin{cases} \frac{1.1060}{1+e^{-(-0.5050t-0.7056)}} + \frac{-3.6388}{1+e^{-(0.7550t-2.7135)}} \\ + \frac{-2.9744}{1+e^{-(-1.0749t+2.0097)}} + \frac{0.9539}{1+e^{-(-0.1283t-0.5130)}} \\ + \frac{-1.0255}{1+e^{-(-0.6703t-2.6204)}} + \frac{-0.8354}{1+e^{-(0.0668t-2.1888)}} \\ + \frac{0.4305}{1+e^{-(0.9271t-0.5100)}} + \frac{-1.0787}{1+e^{-(0.4390t-1.7351)}} \\ + \frac{2.2456}{1+e^{-(-1.1526t+2.1596)}} + \frac{2.6392}{1+e^{-(1.1039t-2.6948)}}, \end{cases} \tag{21}$$

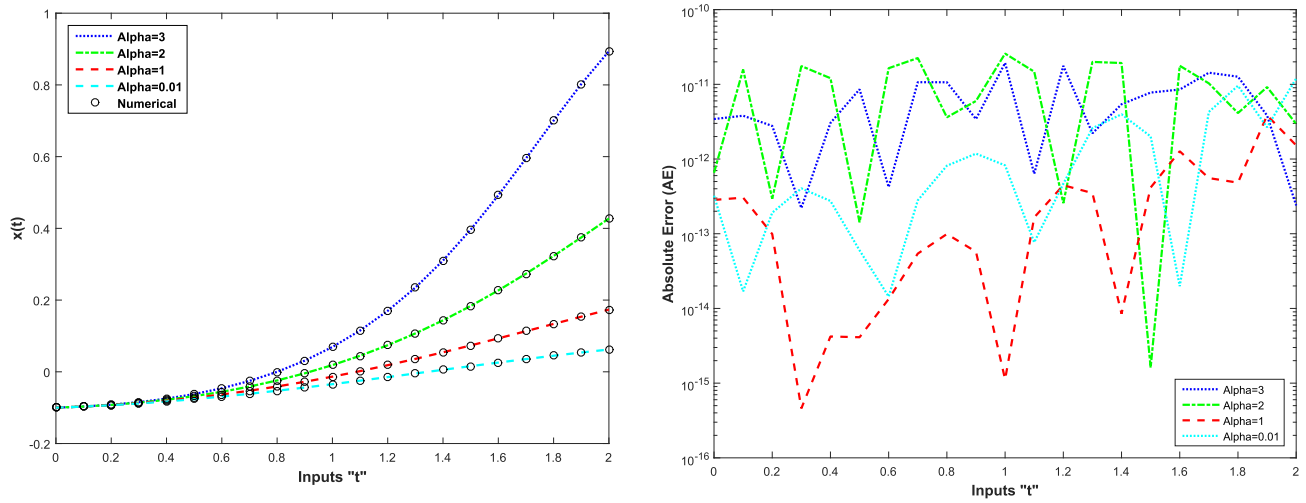

(a) (b)

FIGURE 6. Solutions obtained by our approach are shown in Fig 6(a) and absolute errors are given in Fig 6(b) for four cases of problem 1, scenario-1.

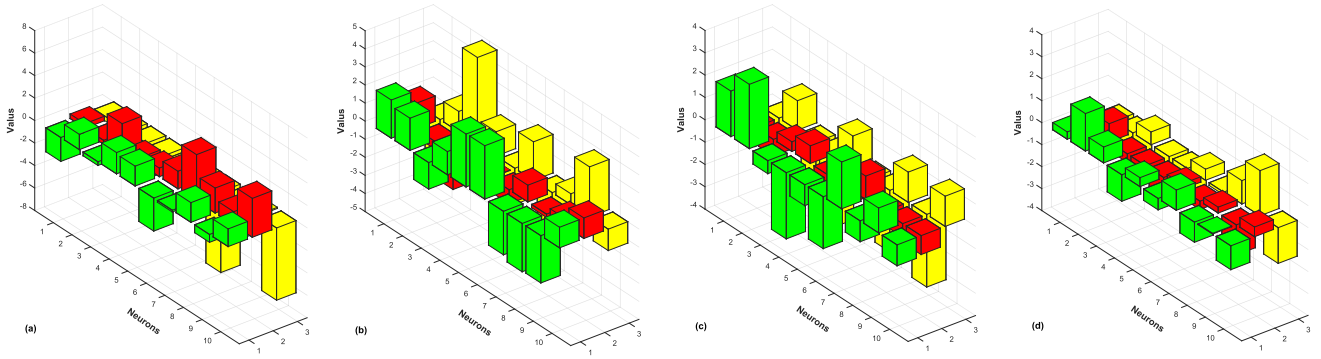

(a) (b) (c) (d)

FIGURE 7. Trained weights for ANNs model optimized through hybrid scheme for cases C_1, C_2, C_3 and C_4 based on variation in α for problem 1, scenario-1.

$$\hat{x}_{c4} = \begin{cases} \frac{0.8117}{1+e^{-(-0.5662t+2.4732)}} + \frac{0.8259}{1+e^{-(-0.8180t+0.1691)}} \\ + \frac{-2.1733}{1+e^{-(-0.7388t-1.7488)}} + \frac{-3.7141}{1+e^{-(0.3526t-0.8723)}} \\ + \frac{-1.5319}{1+e^{-(-0.0161t-1.4839)}} + \frac{1.2671}{1+e^{-(-0.1666t+1.6901)}} \\ + \frac{1.5969}{1+e^{-(0.9643t-2.1267)}} + \frac{-1.8571}{1+e^{-(-0.8267t+0.4666)}} \\ + \frac{2.1674}{1+e^{-(-0.7294t-1.8080)}} + \frac{-0.0025}{1+e^{-(-3.8840t-3.2643)}}, \end{cases} \tag{22}$$

The solution of $\hat{x}_{c_2}$ of scenario-2 is same as the solution of $case_2$ of scenario-1. Suggested solutions are presented in figure (8a) and are formed for inputs in interval $[0, 2]$, and using the step size of $h = 0.1$. However, the results of absolute error for every case are graphically illustrated in figure (8b). It is observed that the proposed hybrid scheme attained the best accuracy of order $10^{-15} - 10^{-11}$.

To obtain the best weights for the ANNs model, fifty independent runs of designed scheme HHO-IPA are performed, and the experimental outcomes are listed in the table (3) in the form of lowest error in solution, worst error in solution, Mean and standard deviation (STD) of errors. It is clear that for these four cases i.e. C_1, C_3 and C_4 the mean values are around $10^{-05} - 10^{-04}$, $10^{-11} - 10^{-10}$ and $10^{-10} - 10^{-09}$. Besides, the accuracy of the designed scheme HHO-IPA is verified by the lower values of STD.

B. PROBLEM-2: VDP DYNAMIC HEARTBEAT MODEL IN THE PRESENCE OF FORCING TERM

Two different scenarios are taken into this problem. Scenario-1 is taken based on changes in pulse shape modification term α while scenario-2 consider the changes in asymmetric damping terms (v_1, v_2) which represent terms associated to the voltage of heartbeat dynamic model (1), with the presence of forcing term $F(t)$ that appears in a normal state of the

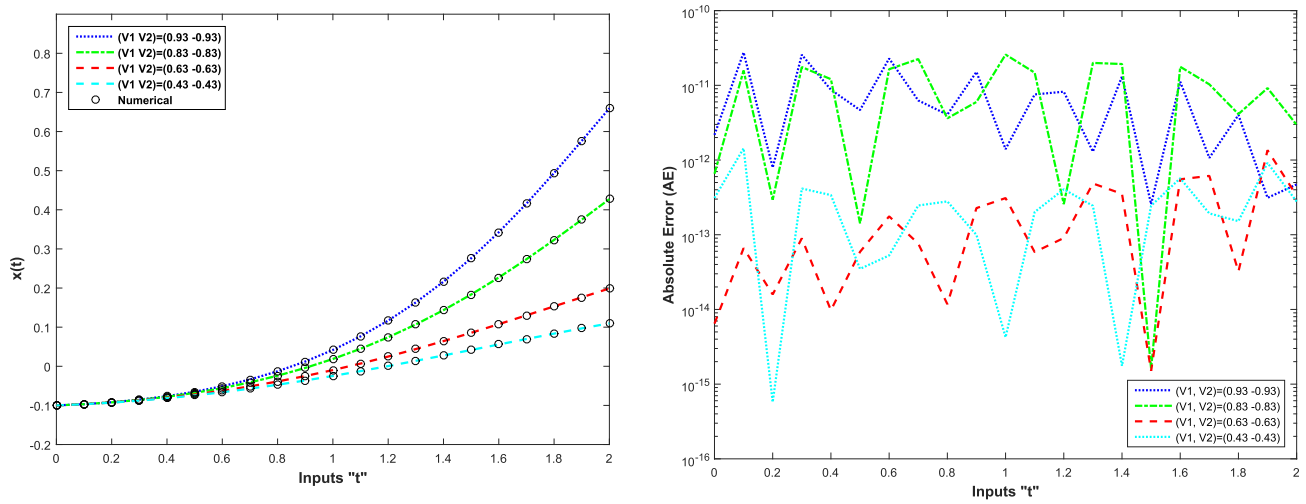

(a) (b)

FIGURE 8. Solutions obtained by our approach are shown in Fig 8(a) and absolute errors are given in Fig 8(b) for four cases of problem 1, scenario-2.

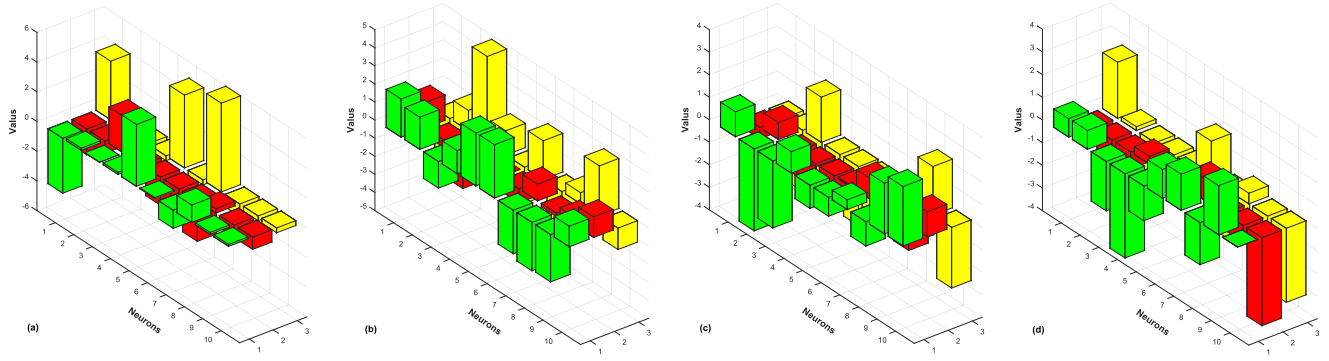

(a) (b) (c) (d)

FIGURE 9. Trained weights for ANNs model optimized through hybrid scheme for cases C_1, C_2, C_3 and C_4 based on variation in asymmetric damping terms (v_1, v_2) for problem 1, scenario-2.

TABLE 3. The statistical analysis of errors of four different cases for scenario-1 and scenario-2 of problem-1, of heartbeat model.

Scenarios	Cases	α	(v_1, v_2)	Best error in solution	Worst error in solution	Mean	STD
Scenario-1	C_1	3	(0.83,-0.83)	6.6486E-12	6.5993E-07	1.7342E-08	9.3016E-08
	C_2	2	(0.83,-0.83)	1.0447E-11	7.1801E-06	2.8539E-07	1.3008E-06
	C_3	1	(0.83,-0.83)	4.7537E-13	2.2572E-04	5.0817E-06	3.1994E-05
	C_4	0.01	(0.83,-0.83)	2.0005E-12	8.4920E-09	1.0183E-09	1.7513E-09
Scenario-2	C_1	2	(0.93,-0.93)	7.9429E-12	3.2799E-04	1.3996E-05	6.5026E-05
	C_2	2	(0.83,-0.83)	1.0447E-11	7.1801E-06	2.8539E-07	1.3008E-06
	C_3	2	(0.63,-0.63)	2.3429E-13	2.5385E-09	5.2768E-10	6.0442E-10
	C_4	2	(0.43,-0.43)	3.0588E-13	1.5198E-08	1.4576E-09	3.4988E-09

natural pacemaker. While d represents the coefficient of cubic factor which switches to harmonic forcing term and the term e in classical VdP equation is constant that is used to control the period of ventricular contraction. Rest of the settings are the same as in problem-1, mathematically forcing term can be represented as follows:

$$F(t) = Asin(\omega t). \tag{23}$$

(a) Scenario-1: Effects of variations in pulse shape modification factor "(α)" of heartbeat model. To analyse the effects of changes in value of "(α)" we considered four cases as follows [58]:

Case 1: Consider Dynamic heartbeat model for $\alpha = 0.5$, $b = 2.5$, $\omega = 1.9$, $e = 6$, $v_1 = 0.97$, $v_2 = -1$ and $d = 3$.

Case 2: Consider heartbeat model for $\alpha = 0.4$, $b = 2.5$, $\omega = 1.9$, $e = 6$, $v_1 = 0.97$, $v_2 = -1$ and $d = 3$.

Case 3: Consider heartbeat model for $\alpha = 0.3$, $b = 2.5$, $\omega = 1.9$, $e = 6$, $v_1 = 0.97$, $v_2 = -1$ and $d = 3$.

Case 4: Consider heartbeat model for $\alpha = 0.2$, $b = 2.5$, $\omega = 1.9$, $e = 6$, $v_1 = 0.97$, $v_2 = -1$ and $d = 3$.

The VdP equation derived from (1) for this scenario with initial conditions is following:

$$\begin{cases} \ddot{x}+\alpha(x+1)(x-0.97)\dot{x} + \dfrac{x(x+6)(x+3)}{6\times 3} = 2.5sin(1.9t), \\ x(0) = -0.1 \quad and \quad \dot{x}(0) = 0.025, \end{cases} \tag{24}$$

for α equal to 0.5, 0.4, 0.3 and 0.2 we analyse the model by four cases C_1, C_2, C_3 and C_4 respectively. Equation (24) is used for this scenario.

Adams numerical technique is used to calculate reference solutions for the second order ODE (24). Exact solutions are not available for this case. We have used same experimental settings as in previous scenarios. The fitness function for this scenario is given as:

$$\begin{aligned} \varepsilon = \frac{1}{N}\sum_{m=1}^{N}\Bigg(&\ddot{\hat{x}}_m + \alpha(\hat{x}_m+1)(\hat{x}_m-0.97)\dot{\hat{x}}_m \\ &+ \frac{\hat{x}_m(\hat{x}_m+6)(\hat{x}_m+3)}{6\times 3}\Bigg)^2 - 2.5\times sin(1.9\times t) \\ &+ \frac{1}{2}\left((\hat{x}_0+0.1)^2 + (\dot{\hat{x}}_0 - 0.025)^2\right). \end{aligned} \tag{25}$$

We have obtained the fitness values for problem-2 scenario-1 as 2.8836×10^{-10}, 2.7479×10^{-10}, 8.0300×10^{-11} and 2.7565×10^{-11} for a set of best weights respectively, for cases C_1, C_2, C_3 and C_4. We have graphically illustrated the ranges of these weights, see figure (11). Series solutions obtained by using best weights which we have obtained for this scenario are given in (26-29):

$$\hat{x}_{c_1} = \begin{cases} \dfrac{0.7467}{1+e^{-(2.1014t-0.1162)}} + \dfrac{-1.0405}{1+e^{-(-3.1418t+3.7057)}} \\ + \dfrac{-2.4484}{1+e^{-(1.9932t-0.2220)}} + \dfrac{1.7577}{1+e^{-(2.7727t+2.5359)}} \\ + \dfrac{0.7248}{1+e^{-(-0.4597t-1.4897)}} + \dfrac{1.3928}{1+e^{-(3.5827t-4.9314)}} \\ + \dfrac{2.2016}{1+e^{-(-1.9035t+3.7091)}} + \dfrac{-2.5529}{1+e^{-(-2.1821t+2.0883)}} \\ + \dfrac{0.2727}{1+e^{-(0.4013t-3.9512)}} + \dfrac{-5.1389}{1+e^{-(2.6355t-7.9241)}}, \end{cases} \tag{26}$$

$$\hat{x}_{c_2} = \begin{cases} \dfrac{-2.7338}{1+e^{-(1.6550t-2.7291)}} + \dfrac{2.3154}{1+e^{-(2.1562t-1.6082)}} \\ + \dfrac{-6.4876}{1+e^{-(2.3027t-7.1152)}} + \dfrac{2.5692}{1+e^{-(2.4369t+2.4153)}} \\ + \dfrac{2.4003}{1+e^{-(2.6334t-3.0941)}} + \dfrac{-0.2154}{1+e^{-(-0.5292t-0.4531)}} \\ + \dfrac{0.1146}{1+e^{-(1.3681t+0.8648)}} + \dfrac{0.8287}{1+e^{-(-0.8645t-0.6892)}} \\ + \dfrac{-1.9497}{1+e^{-(-3.2408t+4.5573)}} + \dfrac{-2.8754}{1+e^{-(1.6017t-0.4486)}}, \end{cases} \tag{27}$$

$$\hat{x}_{c_3} = \begin{cases} \dfrac{-3.4309}{1+e^{-(-2.4260t+2.7255)}} + \dfrac{-1.6307}{1+e^{-(-2.2954t+1.5736)}} \\ + \dfrac{-2.7954}{1+e^{-(1.7471t-1.8331)}} + \dfrac{0.9272}{1+e^{-(-0.4634t-0.3235)}} \\ + \dfrac{-6.5705}{1+e^{-(2.2492t-7.0304)}} + \dfrac{4.0621}{1+e^{-(1.6955t+2.4509)}} \\ + \dfrac{-1.5434}{1+e^{-(-1.9966t-1.8031)}} + \dfrac{2.8419}{1+e^{-(2.9307t+-4.2248)}} \\ + \dfrac{2.6178}{1+e^{-(-1.6184t-0.3252)}} + \dfrac{-2.7630}{1+e^{-(1.4511t-2.6194)}}, \end{cases} \tag{28}$$

$$\hat{x}_{c_4} = \begin{cases} \dfrac{-3.9300}{1+e^{-(-2.5963t+3.8815)}} + \dfrac{1.1808}{1+e^{-(3.3764t+2.8544)}} \\ + \dfrac{2.6626}{1+e^{-(2.1623t-2.3982)}} + \dfrac{-2.3341}{1+e^{-(-0.0228t+0.9476)}} \\ + \dfrac{3.1784}{1+e^{-(-1.2856t+4.4091)}} + \dfrac{0.4512}{1+e^{-(0.4425t+0.7795)}} \\ + \dfrac{0.4893}{1+e^{-(-0.3455t-1.0076)}} + \dfrac{-3.2730}{1+e^{-(1.9483t-3.5433)}} \\ + \dfrac{-4.9540}{1+e^{-(2.3017t-6.9413)}} + \dfrac{1.0879}{1+e^{-(-2.2731t+0.2468)}}. \end{cases} \tag{29}$$

Solutions for this scenario are achieved by using inputs between $[0, 2]$ with a step size of $h = 0.1$. By using our best set of weights we get equations $(26-29)$ and are illustrated in figure (10). The values of AE in our solutions from the reference numerical solution for all cases of problem-2 scenario-1 are given in figure (11). It is obvious that AEs for all cases are achieved of order around $10^{-09} - 10^{-13}$. The statistical analysis of our results is measured in terms of errors in the best solution, worst solution, mean values of absolute errors (AE) and standard deviation (STD). These results are established based on 50 independent runs and are given in table (4). The mean values for cases i.e. C_1, C_2, C_3 and C_4 are around $10^{-09} - 10^{-07}$, $10^{-04} - 10^{-02}$, $10^{-09} - 10^{-07}$ and $10^{-10} - 10^{-08}$. It is worth to note, that the accuracy of our designed scheme HHO-IPA is verified by the lower values of standard deviation in errors for solutions of all cases.

(b) Scenario-2: Effects of variations in asymmetric damping terms (v_1, v_2) on the dynamic heartbeat model.

In this scenario we have studied the effects of variation in asymmetric damping parameters (v_1, v_2) on the heartbeat dynamic model. We have considered four cases for this purpose as follows:

Case 1 Consider Dynamic heartbeat model for $v_2 = -1$, $b = 2.5$, $e = 6$, $\omega = 1.9$, $\alpha = 0.5$ and $v_1 = 0.97$, $d = 3$.

Case 2 Consider Dynamic heartbeat model for $v_2 = -3$, $b = 2.5$, $e = 6$, $\omega = 1.9$, $\alpha = 0.5$ and $v_1 = 0.87$, $d = 3$.

Case 3 Consider Dynamic heartbeat model for $v_2 = -4$, $b = 2.5$, $e = 6$, $\omega = 1.9$, $\alpha = 0.5$ and $v_1 = 0.67$, $d = 3$.

Case 3 Consider Dynamic heartbeat model for $v_2 = -5$, $b = 2.5$, $e = 6$, $\omega = 1.9$, $\alpha = 0.5$ and $v_1 = 0.47$, $d = 3$.

The mathematical model of VdP and corresponding initial conditions for this scenario is given as:

$$\begin{cases} \ddot{x} + 0.5(x-v_2)(x-v_1)\dot{x} + \dfrac{x(x+3)(x+6)}{3\times 6} \\ \qquad = 2.5\times sin(t\times 1.9), \\ x(0) = -0.1 \quad and \quad \dot{x} = 0.025, \end{cases} \tag{30}$$

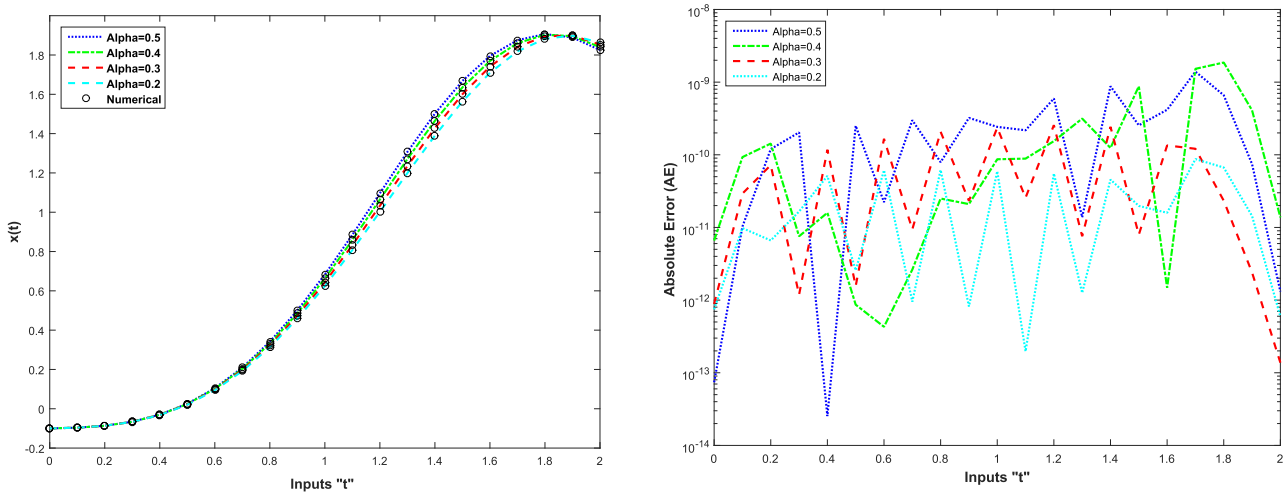

(a) (b)

FIGURE 10. Solutions obtained by our approach are shown in Fig 10(a) and absolute errors are given in Fig 10(b) for four cases of problem 2, scenario-1.

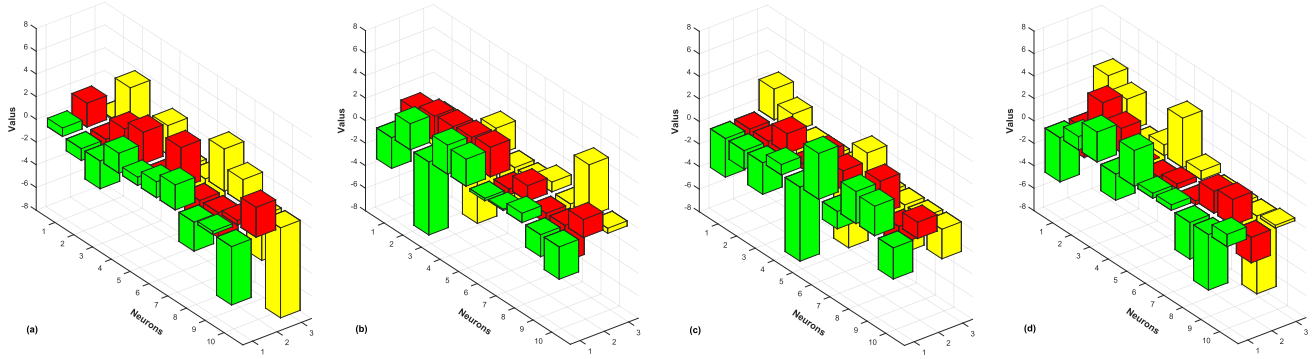

(a) (b) (c) (d)

FIGURE 11. Trained weights for ANNs model optimized through hybrid scheme for cases C_1, C_2, C_3 and C_4 based on variation in α for problem 2, scenario-1.

replacing $(v_1, v_2) = (0.97, -1), (0.87, -3), (0.67, -4)$ and $(0.47, -5)$, in equation (30 we get cases C_1, C_2, C_3 and C_4, of this scenario, respectively.

Exact solution for the system in equation (24) does not exist in literature; for this reason, approximate solutions of equation (24) are found by using AM, and these solutions are used as reference solutions. We have used the same experimental settings as in previous scenarios. Fitness function for these variations is as follows:

$$\varepsilon = \frac{1}{N}\sum_{m=1}^{N}\left(\ddot{\hat{x}}_m + 0.5(\hat{x}_m - v_2)(\hat{x}_m - v_1)\hat{x}_m + \frac{\hat{x}_m(\hat{x}_m+6)(\hat{x}_m+3)}{6\times 3}\right)^2 - 2.5\times sin(t\times 1.9) + \frac{1}{2}\left((\hat{x}_0 - 0.025)^2 + (\hat{x}_0 + 0.1)^2\right) \tag{31}$$

The set of trained weights optimized through HHO-IPA, respectively for cases C_2, C_3 and C_4 with fitness values 3.6962×10^{-10}, 1.8650×10^{-10} and 2.0357×10^{-10} are graphically represented in figure (13). Using these weights the derived solutions for cases C_2, C_3 and C_4 are mathematically defined as follows:

$$\hat{x}_{c_1} = \begin{cases} \frac{0.7467}{1+e^{-(2.1014t-0.1162)}} + \frac{-1.0405}{1+e^{-(-3.1418t+3.7057)}} \\ + \frac{-2.4484}{1+e^{-(1.9932t-0.2220)}} + \frac{1.7576}{1+e^{-(2.7727t+2.5359)}} \\ + \frac{0.7248}{1+e^{-(-0.4597t-1.4897)}} + \frac{1.3928}{1+e^{-(3.5827t-4.9314)}} \\ + \frac{2.2016}{1+e^{-(-1.9035t+3.7091)}} + \frac{-2.5529}{1+e^{-(-2.1821t+2.0883)}} \\ + \frac{0.2727}{1+e^{-(0.4013t-3.9512)}} + \frac{-5.1389}{1+e^{-(2.6355t-7.9241)}}, \end{cases} \tag{32}$$

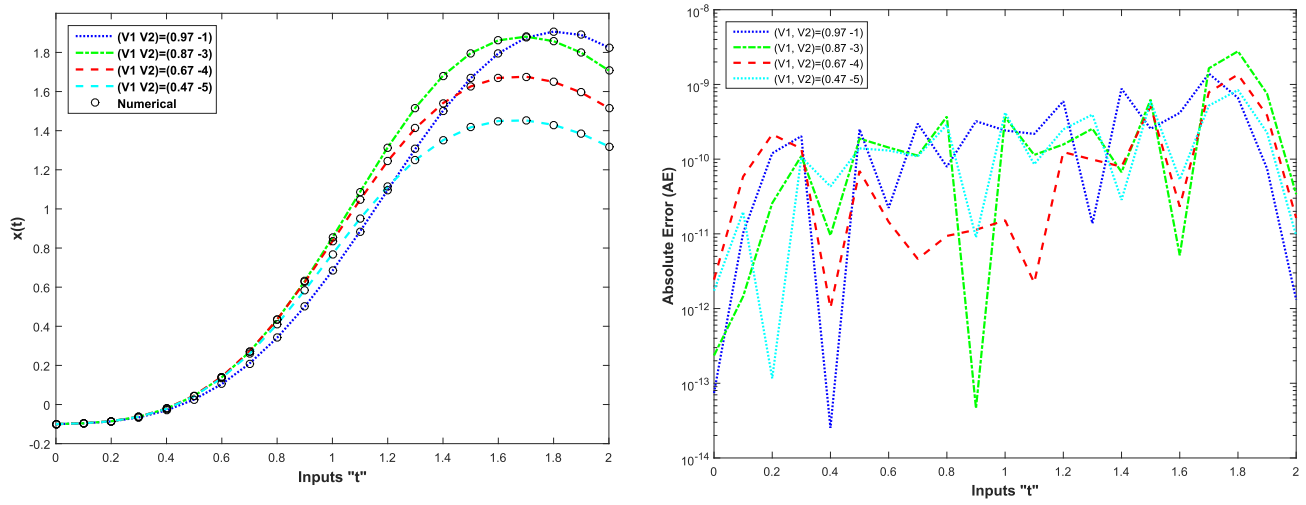

(a) (b)

FIGURE 12. Solutions obtained by our approach are shown in Fig 12(a) and absolute errors are given in Fig 12(b) for four cases of problem 2, scenario-2.

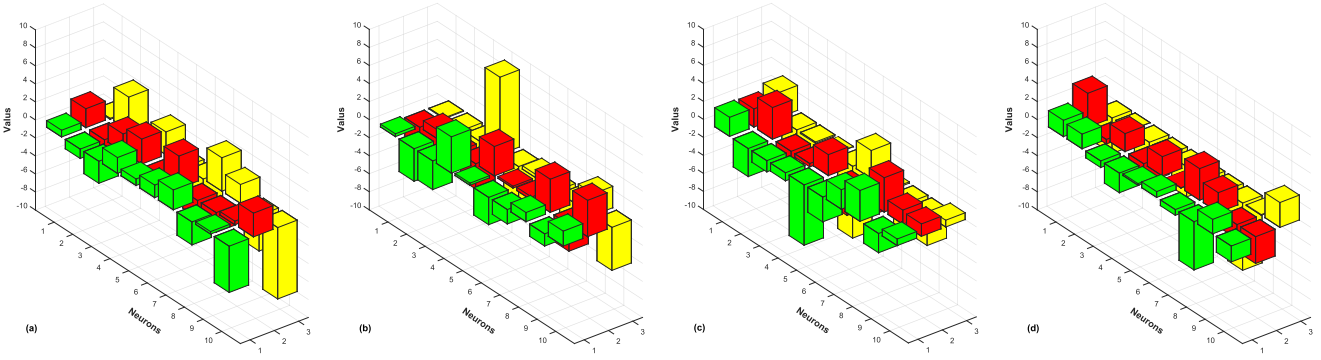

(a) (b) (c) (d)

FIGURE 13. Trained weights for ANNs model optimized through hybrid scheme for cases C_1, C_2, C_3 and C_4 based on variation in asymmetric damping terms (v_1,v_2) for problem-2, scenario-2.

TABLE 4. The statistical analysis of errors for four different cases for scenario-1 and scenario-2 of problem-2, of heartbeat model.

Scenarios	Cases	α	(v_1, v_2)	Best error in solution	Worst error in solution	Mean	STD
Scenario-1	C_1	0.5	(0.97,-1)	2.8836E-10	6.6261E-08	1.2908E-08	1.3785E-08
	C_2	0.4	(0.97,-1)	2.7479E-10	2.4219E-08	5.8951E-09	6.1479E-09
	C_3	0.3	(0.97,-1)	8.0300E-11	9.7161E-09	2.2891E-09	2.7488E-09
	C_4	0.2	(0.97,-1)	2.7565E-11	2.2436E-08	2.8613E-09	5.1755E-09
Scenario-2	C_1	0.5	(0.97,-1)	2.8836E-10	2.5547E-06	3.6693E-08	2.5460E-07
	C_2	0.5	(0.87,-3)	3.6962E-10	8.5945E-08	2.2093E-08	2.3081E-08
	C_3	0.5	(0.67,-4)	1.8650E-10	9.1357E-10	1.8537E-08	2.0247E-08
	C_4	0.5	(0.47,-5)	2.0358E-10	2.8389E-07	3.7522E-08	4.5560E-08

$$\hat{x}_{c_2} = \begin{cases} \frac{0.3091}{1+e^{-(-2.6845t-0.0899)}} + \frac{-3.5999}{1+e^{-(0.9953t-1.5538)}} \\ + \frac{-3.1778}{1+e^{-(-1.9091t-2.2014)}} + \frac{4.0139}{1+e^{-(-2.7938t+8.5594)}} \\ + \frac{0.2328}{1+e^{-(3.2578t-5.3330)}} + \frac{-3.0240}{1+e^{-(0.2102t+0.3699)}} \\ + \frac{-1.5976}{1+e^{-(0.3611t-1.3396)}} + \frac{1.01746}{1+e^{-(3.6784t-3.7313)}} \\ + \frac{-1.3492}{1+e^{-(-2.9540t+2.3764)}} + \frac{1.6509}{1+e^{-(4.0286t-4.7675)}}, \end{cases} \tag{33}$$

$$\hat{x}_{c_3} = \begin{cases} \frac{2.1160}{1+e^{-(2.0180t+2.7664)}} + \frac{-3.1155}{1+e^{-(3.5157t-4.0161)}} \\ + \frac{-1.2446}{1+e^{-(-1.02256t-0.1344)}} + \frac{-0.8967}{1+e^{-(-0.3769t+0.0366)}} \\ + \frac{-6.6985}{1+e^{-(2.3287t-7.9767)}} + \frac{-2.7543}{1+e^{-(-3.0748t+3.1021)}} \\ + \frac{2.1647}{1+e^{-(-1.9743t+0.1478)}} + \frac{3.4242}{1+e^{-(3.8073t-4.2497)}} \\ + \frac{-2.1390}{1+e^{-(1.559t-3.4066)}} + \frac{0.7325}{1+e^{-(1.3713t+0.7520)}}, \end{cases} \tag{34}$$

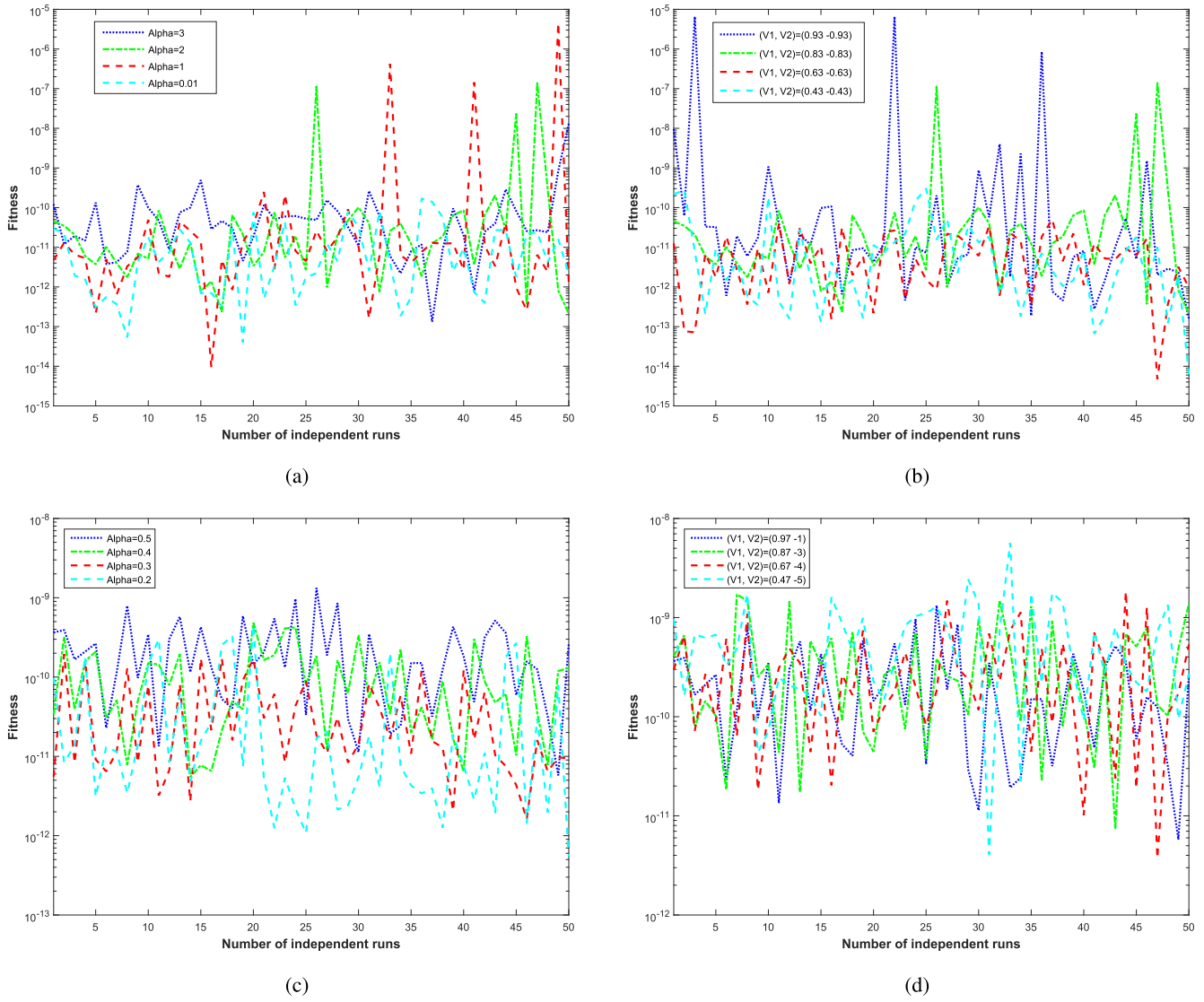

FIGURE 14. The graphs of fitness values for every case of both problems for fifty independent runs of heartbeat model. (a) and (c) shows scenario-1 of problem-1 and problem-2 for unlike values of α respectively, while (b) and (d) shows scenario-2 of problem-1 and problem-2 for unlike values of (v_1, v_2).

$$\hat{x}_{c_4} = \begin{cases} \frac{1.8071}{1+e^{-(3.7645t-3.9468)}} + \frac{1.6267}{1+e^{-(-0.5002t-0.0036)}} \\ + \frac{-0.7320}{1+e^{-(1.9901t-4.3959)}} + \frac{-2.1784}{1+e^{-(-2.3896t-2.1521)}} \\ + \frac{0.1828}{1+e^{-(2.1332t-3.3589)}} + \frac{0.6432}{1+e^{-(0.0422t-1.4856)}} \\ + \frac{-0.6390}{1+e^{-(3.5042t-4.1228)}} + \frac{-5.3473}{1+e^{-(2.1846t-7.4540)}} \\ + \frac{1.6060}{1+e^{-(-1.5835t+0.0701)}} + \frac{-1.7584}{1+e^{-(-2.9690t+2.7533)}}. \end{cases} \tag{35}$$

Best solution of $\hat{x}_{c_1}$ in the present scenario and $\hat{x}_{c_1}$ in previous scenario are similar. We got our results based on the inputs in the interval $[0, 2]$ with $h = 0.1$ taken as step size and the AE in our solutions and reference numerical solutions are given in figure (13). It is evident that the accuracy of the order between $10^{-11} - 10^{-07}$ is achieved by our designed technique. Fifty independent runs are simulated based on our hybrid scheme HHO-IPA. Our experimental outcomes are presented in terms of the best error in solution, worst error in solution, STD and Mean of error which is listed in the table (4). It is observed that the mean values for these three cases i.e. C_2, C_3 and C_4, respectively are of order $10^{-05} - 10^{-06}$, $10^{-04} - 10^{-06}$ and $10^{-04} - 10^{-05}$. Additionally, lower values of standard deviation revealed the exactness of our proposed scheme.

V. DISCUSSION ON RESULTS

In this research, we have considered a VdP heartbeat model see figure (4). It is a second-order, non-linear ordinary differential equation with initial conditions. Our analysis is divided into two main problems and sixteen subcases, see figure (4).

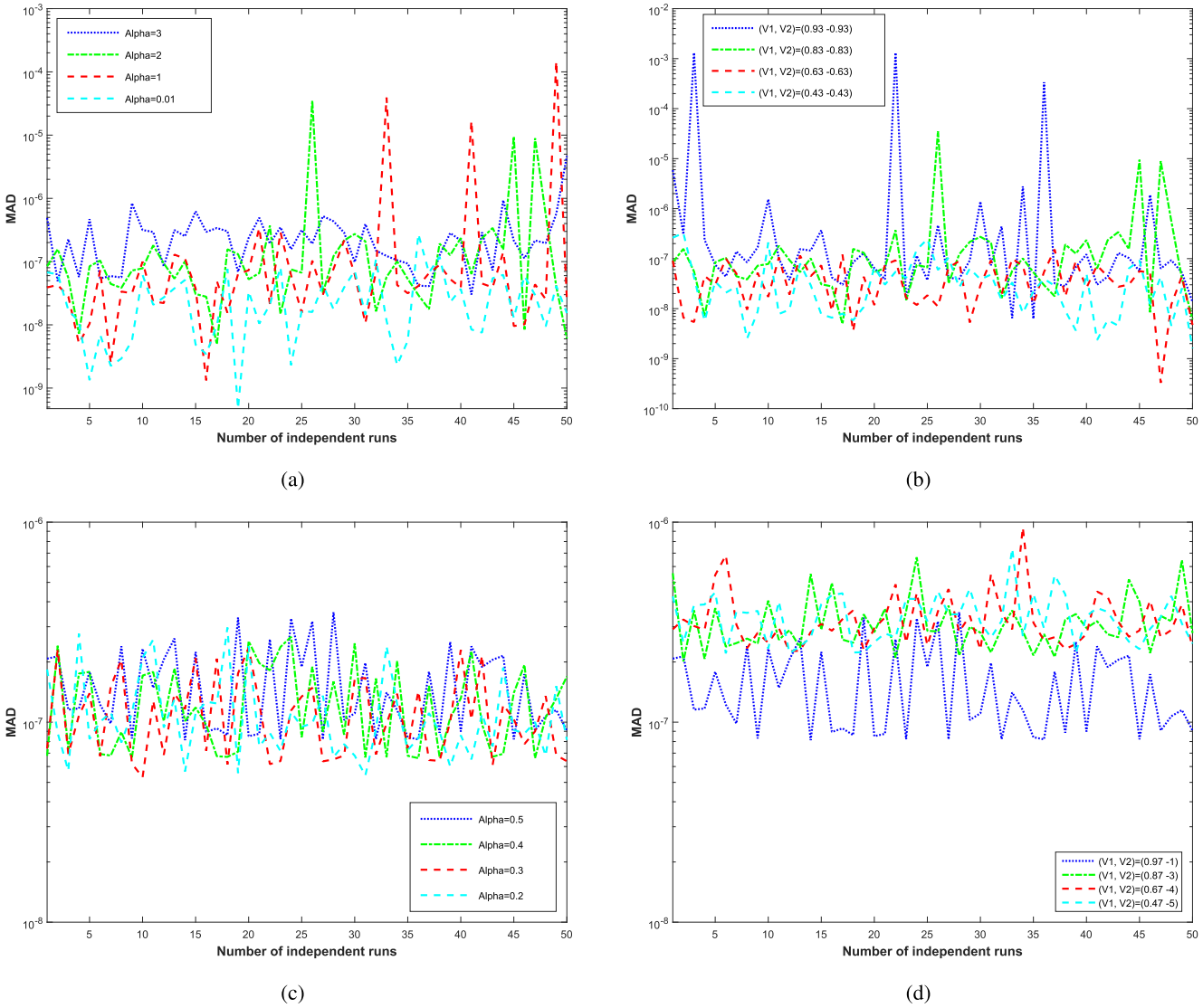

FIGURE 15. The graph of MAD values considering sixteen cases of HBM for fifty independent runs of heartbeat model. (a) and (c) shows scenario-1 of problem-1 and problem-2 for unlike values of α respectively, while (b) and (d) shows scenario-2 of problem-1 and problem-2 for unlike values of (v_1, v_2).

TABLE 5. Convergence complexity for the proposed algorithm based on performance indicators for every change in heartbeat model.

Problem	Scenario	Cases	$Cr_{FIT}(10^{-xx})$			$Cr_{MAD}(10^{-xx})$			$Cr_{RMSE}(10^{-xx})$			$Cr_{ENSE}(10^{-xx})$		
			05	07	09	03	05	07	03	05	06	05	07	09
P-1	S-1	C_1	50	50	44	50	49	00	50	49	18	50	50	49
		C_2	50	47	45	50	47	07	50	47	05	50	47	46
		C_3	49	47	45	50	47	09	50	47	44	48	47	45
		C_4	50	50	50	50	50	25	50	50	47	50	50	49
	S-2	C_1	48	47	40	47	45	04	47	43	35	47	47	42
		C_3	50	50	50	50	50	19	50	50	50	50	50	50
		C_4	50	50	47	50	50	19	50	50	46	50	50	46
P-2	S-1	C_1	50	50	29	50	50	00	50	50	26	50	50	50
		C_2	50	50	41	50	50	00	50	50	30	50	50	50
		C_3	50	50	50	50	50	00	50	50	40	50	50	50
		C_4	50	50	45	50	50	00	50	50	42	50	50	50
	S-2	C_2	50	50	21	50	50	00	50	50	00	50	50	50
		C_3	50	50	23	50	50	00	50	50	00	50	50	50
		C_4	50	50	12	50	50	00	50	50	00	50	50	50

Below we present details of our experimental outcome in this paper:

A. PROBLEM-I, SCENARIO-I

In this scenario, we have analyzed the effects of variations in pulse shape modification factor α in heartbeat model. We have subdivided this scenario into four cases by choosing different values of α. It is worth noting, that the exact solution doesn't exist for equation (12). Results obtained by RKM are used as reference solutions. It is observed that results obtained by our hybrid scheme of ANNs and HHO-IPA are better than RKM solutions. Our results for C_1, C_2, C_3, and C_4

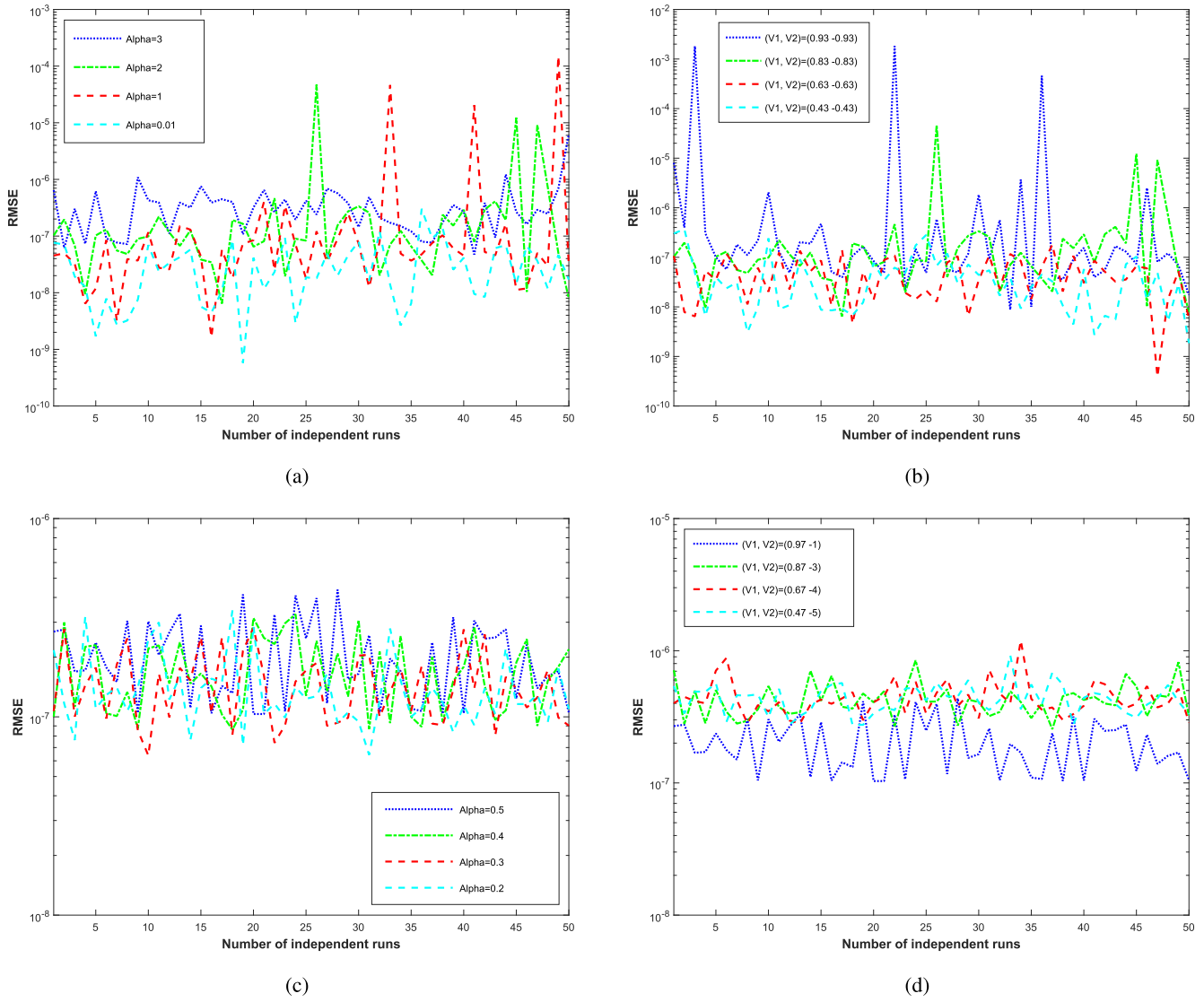

FIGURE 16. The graph of RMSE values considering sixteen cases of HBM for fifty independent runs of heartbeat model. (a) and (c) shows scenario-1 of problem-1 and problem-2 for unlike values of α respectively, while (b) and (d) shows scenario-2 of problem-1 and problem-2 for unlike values of (v_1, v_2).

are 6.6486E-12, 1.0447E-11, 4.7537E-13, and 2.0005E-12 respectively, see figure (6b). These solutions are obtained by using the best weights obtained by our optimizer the HHO-IPA, see figure (7). As in figure (6b), solutions for $\alpha = 1$ are best in terms of residual errors. On the other hand, solutions at $\alpha = 2, 3$ are comparatively worse. For $\alpha = 0.001$, we got average solutions. This means that higher values of pulse shape modification factor results in exponentially growing solutions, see figure (6a).

B. PROBLEM-I, SCENARIO-II

In this scenario, we have analyzed the effects of variations in asymmetric damping terms (v_1, v_2) on the dynamic heartbeat model in the absence of forcing term. Four subcases are considered by varying values of (v_1, v_2). The exact solution to this problem is not known. We have considered the solutions obtained by Adam's numerical technique as reference solutions. The same experimental settings are used as in scenario-I. After training weights of ANNs, our optimizer HHO-IPA, successfully got better solutions with lower errors. Fitness values of our solutions for C_1, C_3, and C_4 are 7.9429E-12, 2.3429E-13, and 3.0588E-13 respectively, see figure (8). In all four cases, errors are in the range of E-15 to E-11. Moreover, the graphs of our solutions are similar with slight variations. This points to the better conditionality of the mathematical heartbeat model. Best, mean, worst, and standard deviations in our errors are listed in the table (3). The best weights for this scenario are given in figure (9).

C. PROBLEM-II, SCENARIO-I

In this problem, the forcing term is considered. It is given in equation (23). In scenario-I, we study the effects of pulse shape modification factor α. We have considered four subcases for different values of α. The mathematical model

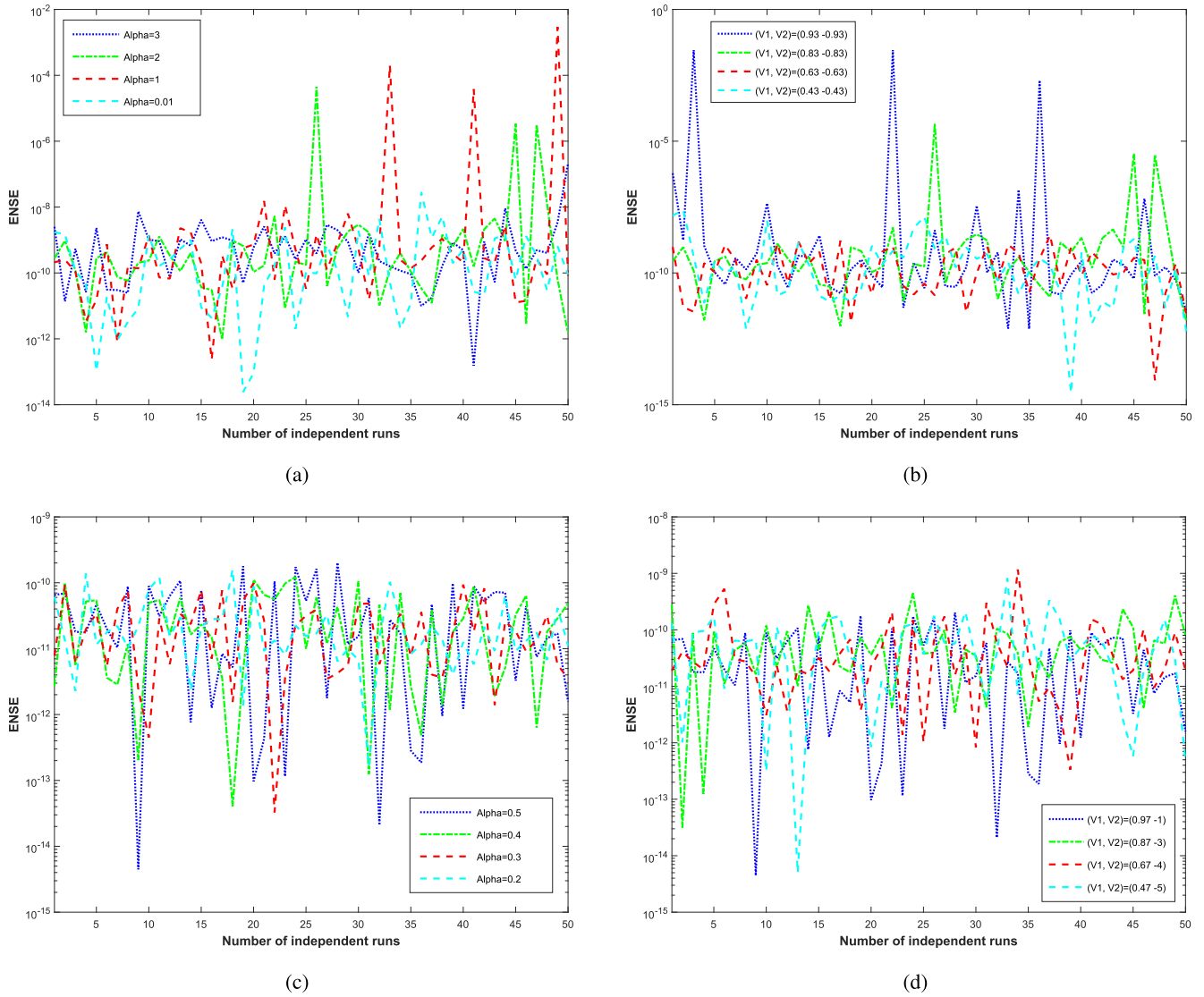

FIGURE 17. The graphs of ENSE considering sixteen cases of HBM for fifty independent runs of heartbeat model. (a) and (c) shows scenario-1 of problem-1 and problem-2 for unlike values of α respectively, while (b) and (d) shows scenario-2 of problem-1 and problem-2 for unlike values of (v_1, v_2).

for this scenario is given in equation (24). As there is no exact solution for this problem, so we have considered solutions obtained by Adam's numerical technique as reference solutions. The same experimental setup is used as in previous scenarios. We have obtained better fitness values for C_1, C_2, C_3, and C_4 as 2.8836E-10, 2.7479E-10, 8.0300E-11, and 2,7565E-11. These errors are graphically illustrated in figure (10) and corresponding weights are shown in figure (11). It is obvious from our experiments that errors in our solutions are lower and are ranging between E-13 and E-10. It is interesting to note that with forcing term solutions are almost similar for all four cases, see figure (10a).

D. PROBLEM-II, SCENARIO-II

In this scenario, we have kept values of α constant, and analyzed the effects of variations in (v_1, v_2) on the heartbeat model in the presence of forcing term. For this purpose, we have considered four cases. Reference solutions by Adam's technique are used for calculating errors in our results. The set of trained weights optimized through HHO-IPA, respectively for cases C_2, C_3, and C_4 are shown in figure (13). We have plotted our solutions in figure (12a). It is observed that there are variations in solution graphs for different values of (v_1, v_2). This points to the significance of terms (v_1, v_2) in the heartbeat model in presence of forcing term. Absolute errors are given in figure (12b), where for all cases errors in our solutions are ranging between E-13 to E-09. Detailed statistical analysis of absolute errors in our solutions are given in table (4).

VI. COMPARATIVE PERFORMANCE-INDEX TESTS

In this section, we have analysed our experimental outcome base on performance indicators as given in equations (36-39), and (40-43). These indicators have further revealed the better

TABLE 6. Convergence complexity for the proposed algorithm based on global performance indicators for every change in heartbeat model.

Problem	Scenario	Cases	Gb_{FIT}		Gb_{MAD}		Gb_{RMSE}		Gb_{ENSE}	
			Mean	STD	Mean	STD	Mean	STD	Mean	STD
P-1	S-1	C_1	3.4684E-10	1.8603E-09	3.4689E-07	6.5554E-07	4.5802E-07	8.8307E-07	5.4048E-09	3.0314E-08
		C_2	5.7078E-09	2.6016E-08	1.1774E-06	5.2350E-06	1.4989E-06	6.9023E-06	1.0269E-06	6.3530E-06
		C_3	1.0163E-07	6.3987E-07	4.0972E-06	2.1330E-05	4.3935E-06	2.2124E-05	6.3463E-05	4.1505E-04
		C_4	2.0366E-11	3.5027E-11	3.5677E-08	4.0765E-08	5.0298E-08	5.0298E-08	1.1932E-09	4.0733E-09
	S-2	C_1	2.7992E-07	1.3005E-07	5.9548E-05	2.6248E-04	8.2296E-05	3.6333E-04	4.2444E-05	2.9392E-04
		C_3	1.0554E-11	1.2088E-11	4.6992E-08	3.7813E-08	5.5285E-08	4.4522E-08	4.1877E-10	5.5951E-10
		C_4	2.9152E-11	6.9976E-11	5.0076E-08	7.0575E-08	5.7294E-08	8.0962E-08	1.6669E-09	4.5278E-09
P-2	S-1	C_1	2.5815E-10	2.7569E-10	1.5904E-07	7.8847E-08	2.0894E-07	9.5420E-08	4.4907E-11	5.1973E-11
		C_2	1.1790E-10	1.2296E-10	1.3077E-07	6.2412E-08	1.7440E-07	7.2530E-08	3.3587E-11	3.4316E-11
		C_3	4.5783E-11	5.4976E-11	1.1538E-07	5.4058E-08	1.4923E-07	6.0747E-08	2.7072E-11	2.7843E-11
		C_4	5.7226E-11	1.0351E-10	1.1424E-07	6.0186E-08	1.4306E-07	6.5825E-08	2.8581E-11	3.5871E-11
	S-2	C_2	4.4185E-10	4.6161E-10	3.2257E-07	1.0926E-07	4.3560E-07	1.3646E-07	7.8425E-11	9.6537E-11
		C_3	3.7074E-10	4.0495E-10	3.3662E-07	1.2918E-07	4.5115E-07	1.6242E-07	8.3333E-11	1.8417E-10
		C_4	7.5044E-10	9.1121E-10	3.4208E-07	9.9355E-08	4.4256E-07	1.2187E-07	8.3680E-11	1.2748E-10

TABLE 7. Computational complexity analysis results for various changes in heartbeat model.

Problem	Scenario	Cases	Time		Population Creations		Function evaluations	
			Mean	STD	Mean	STD	Mean	STD
P-1	S-1	C_1	38.3	2.1	1578.0	36.7	72,490.4	1671.7
		C_2	38.1	2.9	1547.9	67.0	73,456.9	3201.1
		C_3	38.2	2.1	1588.9	17.3	73,204.9	2967.3
		C_4	38.8	5.8	1538.7	57.4	71,937.7	4572.1
	S-2	C_1	38.1	2.1	1573.6	03.7	78,673.8	921.4
		C_3	38.2	1.9	1589.5	24.1	74,765.5	2908.5
		C_4	39.3	6.9	1529.0	114.7	73,724.0	7232.1
P-2	S-1	C_1	38.7	2.0	1550.0	02.6	74,536.2	21.3
		C_2	39.2	2.2	1590.8	04.8	72,951.4	211.2
		C_3	39.2	2.1	1584.3	09.0	73,657.8	301.8
		C_4	39.3	2.4	1591.4	00.0	76,847.8	721.8
	S-2	C_2	39.9	2.1	1573.7	00.0	75,939.3	1029.2
		C_3	38.4	2.7	1576.9	38.1	74,573.9	2192.7
		C_4	38.5	2.8	1580.0	23.7	73,948.0	2900.0

convergence and accuracy of our designed soft computing technique.

Mathematical expressions for mean absolute derivation (MAD), root-mean-square error (RMSE) and error in Nash–Sutcliffe efficiency (ENSE) are given as follows:

$$MAD = \frac{1}{N}\sum_{m=1}^{N}\left(|\hat{x}(t_i) - x(t_i)|\right), \tag{36}$$

$$RMSE = \sqrt{\frac{1}{N}\sum_{m=1}^{N}\left(\hat{x}(t_i) - x(t_i)\right)^2}, \tag{37}$$

$$NSE = 1 - \left(\frac{\sum_{i=1}^{N}(\hat{x}(t_i) - x(t_i))^2}{\sum_{i=1}^{N}(x(t_i) - \frac{1}{N}\sum_{i=1}^{N}(x(t_i)))^2}\right), \tag{38}$$

$$ENSE = |1 - NSE|. \tag{39}$$

The values of performance indicators containing fitness, ENSE, MAD, and RMSE for fifty independent runs are calculated, and the consistency and effectiveness of the designed computing approach are inspected.

Graphical illustrations of MAD,fitness, ENSE and RMSE respectively are presented on semi-log scale for 50 runs, see figures (14), (15), (16) and (17).

It is observed that different values of MAD, RMSE and ENSE performance indicators varied directly with fluctuations in fitness values between low and high. It is noted that for problem-1 scenario-1, and C_1 these variations are negligible as seen from values of MAD, ENSE and RMSE. Additionally, for mentioned case the value of these indicators are comparatively decreased. Reliability of our designed technique is further inspected through by percentage of converged runs on the basis of pre-described criterion of MAD, fitness, ENSE and RMSE values. The successfully converged runs (Cr) for fifty separate simulations is calculated for each case and our results are tabulated in table (5) for both problems. These calculations are done based on the following criteria, i.e. $(Cr_{FIT}) \leq E-07$, $(Cr_{MAD}) \leq E-05$, $(Cr_{RMSE}) \leq E-05$ and $(Cr_{ENSE}) \leq E-07$. It is interesting to note that the average rate of convergence of our scheme is almost 100%.

Further estimation of the performance of our designed technique is carried out by describing its efficiency through global indicators, i.e.global MAD, global RMSE, global ENSE and global fitness. Formulations for these indicators are following:

$$Gb_{MAD} = \frac{1}{R_n}\sum_{r=1}^{R_n}\left(\frac{1}{G_p}\sum_{i=1}^{G_p}|\hat{x}_r(t_i) - x(t_i)|\right), \tag{40}$$

$$Gb_{RMSE} = \frac{1}{R_n}\sum_{r=1}^{R_n}\left(\sqrt{\frac{1}{G_p}\sum_{i=1}^{G_p}(\hat{x}(t_i) - x(t_i))^2}\right), \tag{41}$$

TABLE 8. Notations and abbreviations used in this paper.

Abbreviation	Description
ANNs	Artificial neural networks
HHO	Harris Hawks Optimizer
IPA	Interior Point Algorithm
VdP	Van der Pol
MAD	Mean absolute deviation
RMSE	Root-mean-square error
AE	Absolute error
AM	Adams method
HBM	Heart beat model
ζ	log-sigmoid function
NSE	Nash–Sutcliffe efficiency
ENSE	Error in Nash–Sutcliffe efficiency
RKM	Runge Kutta Method
FF	Fitness function
STD	Standard deviation
Cr	Converged runs
Gb	Global indicators
Gp	Number of total input values
Rn	Number of total runs
x	Fiber of heart
α	Pulse shape modification factor of heart
v_1, v_2	Asymmetric components for modification of damping terms
e	Duration of ventricular contraction
$F(t)$	External force factor
ODEs	Ordinary differential Equations
ε	Mean squared error
BFGS	Broyden-Fletcher-Goldfarb-Shanno algorithm
CCA	Computational complexity analysis

$$Gb_{ENSE} = \frac{1}{R_n}\sum_{r=1}^{R_n}\left(\frac{\sum_{i=1}^{N}(\hat{x}(t_i)-x(t_i))^2}{\sum_{i=1}^{N}(\frac{1}{N}\sum_{i=1}^{N}(x(t_i))-x(t_i))^2}\right), \quad (42)$$

$$Gb_{FIT} = \frac{1}{R_n}\sum_{r=1}^{R_n}\varepsilon_r, \quad (43)$$

where G_p in above equations is a number of total input values, R_n is number of total executed runs, ε_r is objective value of r^{th} experiment, $\hat{x}(t)$ and $x_r(t)$ are the standard solutions for same number run. The inputs t ϵ [0, 2] with the step size 0.1 are taken in this study, i.e., $G_p = 21$ and $R_n = 50$. Results of Gb_{Fit}, Gb_{MAD}, Gb_{RMSE} and Gb_{ENSE} are listed in Table (6) for all problems. Furthermore, the lower values of global performance indicators for most of the cases shows the coherent accuracy and consistency of HHO-IPA.

Computational complexity analysis (CCA) is performed for the designed algorithm based on average time taken for the calculation of unknown parameters of ANNs by HHO-IPA, the average number of function evaluations and population creation. Values of CCA operators are given in Table (7) together with mean and standard deviation considered for 50 independent runs of designed technique for all case studies of both problems. It is evident that the mean values of population creation, number of function evaluations and time for problem-1 are about 1570, 74, 536 and 38s respectively. While these values for problem-2 are about 1577, 75, 259, and 39s respectively. All calculation and evaluation for this research are done on HP Laptop *AMD A*4 − 4300 *APU with Radeon*(*TM*) *HD Graphics CPU* @2.50 *GHz* 2.50 *GHz*, 8.00 *GB RAM*, 64 *bit operating system*, ×64 *based Processor*, *in Microsoft Windows* 10 *Education edition running R*2015*a version of MATLAB*.

VII. CONCLUSIONS

We conclude this research by stating the following key findings and contributions which are revealed from our experiments:

- A soft computing procedure is designed to analyse the mathematical model of Van der Pol type equations. These equations represent the heartbeat dynamics. Series solutions are constructed with the help of artificial neural networks. Unknown weights are finely tuned by a combination of a global search technique the Harris Hawks Optimizer HHO) and a local search technique the Interior Point Algorithm (IPA) named as HHO-IPA.
- Approximate series solutions of the VdP heartbeat model are proposed and graphically plotted. Our outcome is in strong agreement with the reference solutions. We have considered two scenarios and sixteen different cases to analyse the mathematical model.
- To check the consistency and accuracy of HHO-IPA, we analysed our results by calculating values of performance indicators, like, absolute errors in solutions, mean and standard deviations in errors. Lower values of these indicators suggested that HHO-IPA can tune unknown weights consistently and accurately for all problems considered in this study.
- Values of MAD, ENSE, RMSE, GbMAD, GbENSE, and GbRMSE are calculated based on our outcome. Optimal values of these indicators dictate that we have attained better results for HBM.
- Computational complexity analysis is carried out by considering function evaluations, mean execution time, number of iterations taken to calculate optimal design weights for our problems. In all cases, negligible fluctuations in these values is observed. It indicated that our algorithm is stable and can handle difficult operations by consuming less time.

- Additionally, interested readers can replace different activation functions. Using orthogonal polynomials to construct the weighted series solution is still worth to investigate.
- By our results we have shown that VdP oscillatory model for hear dynamics is a well-conditioned model.
- Our methodology can be implemented to solve problems in biomathematics, and physics.

REFERENCES

[1] K. Grudziński and J. J. Żebrowski, "Modeling cardiac pacemakers with relaxation oscillators," *Phys. A, Stat. Mech. Appl.*, vol. 336, nos. 1–2, pp. 153–162, May 2004.
[2] K. Hall, D. J. Christini, M. Tremblay, J. J. Collins, L. Glass, and J. Billette, "Dynamic control of cardiac Alternans," *Phys. Rev. Lett.*, vol. 78, no. 23, pp. 4518–4521, Jun. 1997.
[3] G. M. Mahmoud, A. A. Farghaly, T. M. Abed-Elhameed, S. A. Aly, and A. A. Arafa, "Dynamics of distributed-order hyperchaotic complex van der Pol oscillators and their synchronization and control," *Eur. Phys. J. Plus*, vol. 135, no. 1, p. 32, Jan. 2020.
[4] A. M. dos Santos, S. R. Lopes, and R. L. R. L. Viana, "Rhythm synchronization and chaotic modulation of coupled Van der Pol oscillators in a model for the heartbeat," *Phys. A, Stat. Mech. Appl.*, vol. 338, nos. 3–4, pp. 335–355, Jul. 2004.
[5] B. B. Ferreira, A. S. de Paula, and M. A. Savi, "Chaos control applied to heart rhythm dynamics," *Chaos, Solitons Fractals*, vol. 44, no. 8, pp. 587–599, Aug. 2011.
[6] G. Gatti, "Statics and dynamics of a nonlinear oscillator with quasi-zero stiffness behaviour for large deflections," *Commun. Nonlinear Sci. Numer. Simul.*, vol. 83, Apr. 2020, Art. no. 105143.
[7] A. K. Shukla, T. R. Ramamohan, and S. Srinivas, "A new analytical approach for limit cycles and quasi-periodic solutions of nonlinear oscillators: The example of the forced van der pol duffing oscillator," *Phys. Scripta*, vol. 89, no. 7, Jul. 2014, Art. no. 075202.
[8] S. A. Alaqel and Y. Q. Hasan, "A novel modification of Adomian decomposition method for singular BVPs of Emden–Fowler type," *J. Adv. Math. Comput. Sci.*, vol. 35, no. 2, pp. 84–100, 2020.
[9] A. Kimiaeifar, A. R. Saidi, A. R. Sohouli, and D. D. Ganji, "Analysis of modified van der Pol's oscillator using He's parameter-expanding methods," *Current Appl. Phys.*, vol. 10, no. 1, pp. 279–283, Jan. 2010.
[10] Y. Khan, M. Madani, A. Yildirim, M. A. Abdou, and N. Faraz, "A new approach to Van der Pol's oscillator problem," *Zeitschrift für Naturforschung A*, vol. 66, nos. 10–11, pp. 620–624, Nov. 2011.
[11] S. S. Motsa and P. Sibanda, "A note on the solutions of the Van der Pol and Duffing equations using a linearisation method," *Math. Problems Eng.*, vol. 2012, pp. 1–10, Sep. 2012.
[12] A. Kimiaeifar, A. Saidi, G. Bagheri, M. Rahimpour, and D. Domairry, "Analytical solution for Van der Pol–duffing oscillators," *Chaos, Solitons Fractals*, vol. 42, no. 5, pp. 2660–2666, 2009.
[13] N. Yadav, A. Yadav, and J. H. Kim, "Numerical solution of unsteady advection dispersion equation arising in contaminant transport through porous media using neural networks," *Comput. Math. Appl.*, vol. 72, no. 4, pp. 1021–1030, Aug. 2016.
[14] N. Yadav, A. Yadav, M. Kumar, and J. H. Kim, "An efficient algorithm based on artificial neural networks and particle swarm optimization for solution of nonlinear Troesch's problem," *Neural Comput. Appl.*, vol. 28, no. 1, pp. 171–178, Jan. 2017.
[15] M. Kumar and N. Yadav, "Multilayer perceptrons and radial basis function neural network methods for the solution of differential equations: A survey," *Comput. Math. Appl.*, vol. 62, no. 10, pp. 3796–3811, Nov. 2011.
[16] W. Waseem, M. Sulaiman, S. Islam, P. Kumam, R. Nawaz, M. A. Z. Raja, M. Farooq, and M. Shoaib, "A study of changes in temperature profile of porous fin model using cuckoo search algorithm," *Alexandria Eng. J.*, vol. 59, no. 1, pp. 11–24, Feb. 2020.
[17] A. H. Bukhari, M. Sulaiman, S. Islam, M. Shoaib, P. Kumam, and M. A. Z. Raja, "Neuro-fuzzy modeling and prediction of summer precipitation with application to different meteorological stations," *Alexandria Eng. J.*, vol. 59, no. 1, pp. 101–116, Feb. 2020.
[18] S. Effati and R. Buzhabadi, "A neural network approach for solving fredholm integral equations of the second kind," *Neural Comput. Appl.*, vol. 21, no. 5, pp. 843–852, Jul. 2012.
[19] M. Kumar and N. Yadav, "Buckling analysis of a beam–column using multilayer perceptron neural network technique," *J. Franklin Inst.*, vol. 350, no. 10, pp. 3188–3204, Dec. 2013.
[20] M. Khalid, M. Sultana, and F. Zaidi, "Numerical solution of sixth-order differential equations arising in astrophysics by neural network," *Int. J. Comput. Appl.*, vol. 107, no. 6, pp. 1–6, 2014.
[21] S. Effati, A. Mansoori, and M. Eshaghnezhad, "An efficient projection neural network for solving bilinear programming problems," *Neurocomputing*, vol. 168, pp. 1188–1197, Nov. 2015.
[22] S. Momani, Z. S. Abo-Hammou, and O. M. K. Alsmad, "Solution of inverse kinematics problem using genetic algorithms," *Appl. Math. Inf. Sci.*, vol. 10, no. 1, pp. 225–233, Jan. 2016.
[23] K. S. McFall, "Automated design parameter selection for neural networks solving coupled partial differential equations with discontinuities," *J. Franklin Inst.*, vol. 350, no. 2, pp. 300–317, Mar. 2013.
[24] J. C. Chedjou and K. Kyamakya, "A universal concept based on cellular neural networks for ultrafast and flexible solving of differential equations," *IEEE Trans. Neural Netw. Learn. Syst.*, vol. 26, no. 4, pp. 749–762, Apr. 2015.
[25] S. Mall and S. Chakraverty, "Application of Legendre neural network for solving ordinary differential equations," *Appl. Soft Comput.*, vol. 43, pp. 347–356, Jun. 2016.
[26] S. Chakraverty and S. Mall, "Regression-based weight generation algorithm in neural network for solution of initial and boundary value problems," *Neural Comput. Appl.*, vol. 25, nos. 3–4, pp. 585–594, Sep. 2014.
[27] S. Mall and S. Chakraverty, "Numerical solution of nonlinear singular initial value problems of Emden–Fowler type using Chebyshev Neural Network method," *Neurocomputing*, vol. 149, pp. 975–982, Feb. 2015.
[28] J. A. Khan, M. A. Z. Raja, M. I. Syam, S. A. K. Tanoli, and S. E. Awan, "Design and application of nature inspired computing approach for nonlinear stiff oscillatory problems," *Neural Comput. Appl.*, vol. 26, no. 7, pp. 1763–1780, Oct. 2015.
[29] S. Mall and S. Chakraverty, "Hermite functional link neural network for solving the Van der Pol–Duffing oscillator equation," *Neural Comput.*, vol. 28, no. 8, pp. 1574–1598, Aug. 2016.
[30] J. Sabouri K., S. Effati, and M. Pakdaman, "A neural network approach for solving a class of fractional optimal control problems," *Neural Process. Lett.*, vol. 45, no. 1, pp. 59–74, Feb. 2017.
[31] A. H. Bukhari, M. A. Z. Raja, M. Sulaiman, S. Islam, M. Shoaib, and P. Kumam, "Fractional neuro-sequential ARFIMA-LSTM for financial market forecasting," *IEEE Access*, vol. 8, pp. 71326–71338, 2020.
[32] A. Sadollah, Y. Choi, D. G. Yoo, and J. H. Kim, "Metaheuristic algorithms for approximate solution to ordinary differential equations of longitudinal fins having various profiles," *Appl. Soft Comput.*, vol. 33, pp. 360–379, Aug. 2015.
[33] M. A. Z. Raja, "Solution of the one-dimensional Bratu equation arising in the fuel ignition model using ANN optimised with PSO and SQP," *Connection Sci.*, vol. 26, no. 3, pp. 195–214, Jul. 2014.
[34] M. Baymani, S. Effati, H. Niazmand, and A. Kerayechian, "Artificial neural network method for solving the Navier–Stokes equations," *Neural Comput. Appl.*, vol. 26, no. 4, pp. 765–773, May 2015.
[35] M. A. Z. Raja, M. A. R. Khan, T. Mahmood, U. Farooq, and N. I. Chaudhary, "Design of bio-inspired computing technique for nanofluidics based on nonlinear Jeffery–Hamel flow equations," *Can. J. Phys.*, vol. 94, no. 5, pp. 474–489, May 2016.
[36] M. A. Z. Raja, U. Farooq, N. I. Chaudhary, and A. M. Wazwaz, "Stochastic numerical solver for nanofluidic problems containing multi-walled carbon nanotubes," *Appl. Soft Comput.*, vol. 38, pp. 561–586, Jan. 2016.
[37] Z. Abo-Hammour, O. A. Arqub, S. Momani, and N. Shawagfeh, "Optimization solution of Troesch's and Bratu's problems of ordinary type using novel continuous genetic algorithm," *Discrete Dyn. Nature Soc.*, vol. 2014, pp. 1–15, 2014.
[38] M. A. Z. Raja, "Stochastic numerical treatment for solving Troesch's problem," *Inf. Sci.*, vol. 279, pp. 860–873, Sep. 2014.
[39] M. A. Z. Raja, J. A. Khan, and T. Haroon, "Stochastic numerical treatment for thin film flow of third grade fluid using unsupervised neural networks," *J. Taiwan Inst. Chem. Eng.*, vol. 48, pp. 26–39, Mar. 2015.
[40] S. Effati and M. H. N. Skandari, "Optimal control approach for solving linear volterra integral equations," *Int. J. Intell. Syst. Appl.*, vol. 4, no. 4, pp. 40–46, Apr. 2012.
[41] M. A. Z. Raja, I. Ahmad, I. Khan, M. I. Syam, and A. M. Wazwaz, "Neuro-heuristic computational intelligence for solving nonlinear pantograph systems," *Frontiers Inf. Technol. Electron. Eng.*, vol. 18, no. 4, pp. 464–484, Apr. 2017.

[42] M. A. Z. Raja, "Numerical treatment for boundary value problems of pantograph functional differential equation using computational intelligence algorithms," *Appl. Soft Comput.*, vol. 24, pp. 806–821, Nov. 2014.
[43] M. A. Z. Raja, J. A. Khan, S. M. Shah, R. Samar, and D. Behloul, "Comparison of three unsupervised neural network models for first Painlevé transcendent," *Neural Comput. Appl.*, vol. 26, no. 5, pp. 1055–1071, Jul. 2015.
[44] M. A. Z. Raja, R. Samar, T. Haroon, and S. M. Shah, "Unsupervised neural network model optimized with evolutionary computations for solving variants of nonlinear MHD Jeffery–Hamel problem," *Appl. Math. Mech.*, vol. 36, no. 12, pp. 1611–1638, Dec. 2015.
[45] M. A. Z. Raja and R. Samar, "Numerical treatment of nonlinear MHD Jeffery–Hamel problems using stochastic algorithms," *Comput. Fluids*, vol. 91, pp. 28–46, Mar. 2014.
[46] Y. Nawaz and M. S. Arif, "Generalized decomposition method: Applications to nonlinear oscillator and MHD fluid flow past cone/wedge geometries," *Numer. Heat Transf. B, Fundamentals*, vol. 77, no. 1, pp. 42–63, Jan. 2020.
[47] M. A. Z. Raja, R. Samar, E. S. Alaidarous, and E. Shivanian, "Bio-inspired computing platform for reliable solution of Bratu-type equations arising in the modeling of electrically conducting solids," *Appl. Math. Model.*, vol. 40, nos. 11–12, pp. 5964–5977, Jun. 2016.
[48] J. A. Khan, M. A. Z. Raja, M. M. Rashidi, M. I. Syam, and A. M. Wazwaz, "Nature-inspired computing approach for solving non-linear singular Emden–Fowler problem arising in electromagnetic theory," *Connection Sci.*, vol. 27, no. 4, pp. 377–396, Oct. 2015.
[49] S. Effati and M. Pakdaman, "Artificial neural network approach for solving fuzzy differential equations," *Inf. Sci.*, vol. 180, no. 8, pp. 1434–1457, Apr. 2010.
[50] G. Gumah, M. F. M. Naser, M. Al-Smadi, S. K. Q. Al-Omari, and D. Baleanu, "Numerical solutions of hybrid fuzzy differential equations in a Hilbert space," *Appl. Numer. Math.*, vol. 151, pp. 402–412, May 2020.
[51] I. Ahmad, M. A. Z. Raja, M. Bilal, and F. Ashraf, "Neural network methods to solve the Lane–Emden type equations arising in thermodynamic studies of the spherical gas cloud model," *Neural Comput. Appl.*, vol. 28, no. S1, pp. 929–944, Dec. 2017.
[52] S. Mall and S. Chakraverty, "Chebyshev neural network based model for solving Lane–Emden type equations," *Appl. Math. Comput.*, vol. 247, pp. 100–114, Nov. 2014.
[53] Z. Sabir, H. A. Wahab, M. Umar, M. G. Sakar, and M. A. Z. Raja, "Novel design of Morlet wavelet neural network for solving second order Lane–Emden equation," *Math. Comput. Simul.*, vol. 172, pp. 1–14, Jun. 2020.
[54] M. A. Z. Raja, M. A. Manzar, and R. Samar, "An efficient computational intelligence approach for solving fractional order Riccati equations using ANN and SQP," *Appl. Math. Model.*, vol. 39, nos. 10–11, pp. 3075–3093, Jun. 2015.
[55] Y. Li, D. Zhao, Y. Chen, I. Podlubny, and C. Zhang, "Finite energy Lyapunov function candidate for fractional order general nonlinear systems," *Commun. Nonlinear Sci. Numer. Simul.*, vol. 78, Nov. 2019, Art. no. 104886.
[56] B. van der Pol and J. van der Mark, "LXXII.The heartbeat considered as a relaxation oscillation, and an electrical model of the heart," *London, Edinburgh, Dublin Phil. Mag. J. Sci.*, vol. 6, no. 38, pp. 763–775, Nov. 1928.
[57] Z.-M. Ge and M.-Y. Hsu, "Chaos in a generalized van der pol system and in its fractional order system," *Chaos, Solitons Fractals*, vol. 33, no. 5, pp. 1711–1745, Aug. 2007.
[58] M. A. Z. Raja, F. H. Shah, and M. I. Syam, "Intelligent computing approach to solve the nonlinear van der pol system for heartbeat model," *Neural Comput. Appl.*, vol. 30, no. 12, pp. 3651–3675, Dec. 2018.
[59] C. Chicone, *Ordinary Differential Equations With Applications*, vol. 34. New York, NY, USA: Springer, 2006.
[60] A. A. Heidari, S. Mirjalili, H. Faris, I. Aljarah, M. Mafarja, and H. Chen, "Harris hawks optimization: Algorithm and applications," *Future Gener. Comput. Syst.*, vol. 97, pp. 849–872, Aug. 2019.
[61] F. A. Potra and S. J. Wright, "Interior-point methods," *J. Comput. Appl. Math.*, vol. 124, nos. 1–2, pp. 281–302, Jan. 2000.
[62] Y. Nesterov and L. Tunçel, "Local superlinear convergence of polynomial-time interior-point methods for hyperbolicity cone optimization problems," *SIAM J. Optim.*, vol. 26, no. 1, pp. 139–170, Jan. 2016.
[63] H. Y. Benson and D. F. Shanno, "Interior-point methods for nonconvex nonlinear programming: Cubic regularization," *Comput. Optim. Appl.*, vol. 58, no. 2, pp. 323–346, Jun. 2014.
[64] D. P. Word, J. K. Young, D. A. T. Cummings, S. Iamsirithaworn, and C. D. Laird, "Interior-point methods for estimating seasonal parameters in discrete-time infectious disease models," *PLoS ONE*, vol. 8, no. 10, 2013, Art. no. e74208.
[65] C. Duan, W. Fang, J. Liu, and L. Jiang, "Adaptive barrier filter-line-search interior point method for optimal power flow with FACTS devices," *IET Gener., Transmiss. Distrib.*, vol. 9, no. 16, pp. 2792–2798, Dec. 2015.

ADNAN KHAN received the bachelor's degree in the combination of maths A, maths B, and physics and the Master of Science degree in mathematics from Abdul Wali Khan University, Mardan, in 2015 and 2017, respectively, where he is currently pursuing the M.Phil. degree in mathematics. His research interests include optimization algorithms, real-world problems, smart grids, communications technology, and energy management.

MUHAMMAD SULAIMAN received the B.Sc. degree from the University of Peshawar, in 2004, the M.Sc. and M.Phil. degrees in mathematics from the Quaid-e-Azam University Islamabad, in 2007 and 2009, respectively, and the Ph.D. degree in mathematics from the University of Essex, U.K., in 2015. From 2009 to 2016, he was a Lecturer in mathematics with Abdul Wali Khan University, Mardan, Pakistan. Since February 2016, he has been an Assistant Professor with the Department of Mathematics, Abdul Wali Khan University. He is the author of two book chapters and more than 15 articles. His research interests include optimization, including mathematical optimization techniques, global optimization, and evolutionary algorithms, heuristics, metaheuristics, multiobjective optimization, design engineering optimization problems, structural engineering optimization problems, linear programming, linear and non-linear least squares optimization problems, evolutionary algorithms, and nature-inspired metaheuristics. He is an Associate Editor of the journal *COJ Reviews and Research*, and *SCIREA Journal of Mathematics*.

HOSAM ALHAKAMI received the B.Sc. degree in computer science from King Abdulaziz University, Saudi Arabia, in 2004, the M.Sc. degree in internet software systems from Birmingham University, Birmingham, U.K., in 2009, and the Ph.D. degree in software engineering from De Montfort University, in 2015. From 2004 to 2007, he worked in the Software Development Industry, where he implemented several systems and solutions for a National Academic Institution. His research interests include algorithms, semantic web, and optimization techniques. He focuses on enhancing real-world matching systems using machine learning and data analytics in the context of supporting decision-making.

AHMAD ALHINDI (Member, IEEE) received the B.Sc. degree in computer science from Umm Al-Qura University (UQU), Mecca, Saudi Arabia, in 2006, and the M.Sc. degree in computer science and the Ph.D. degree in computing and electronic systems from the University of Essex, Colchester, U.K., in 2010 and 2015, respectively. He is currently an Assistant Professor of artificial intelligence (AI) with the Computer Science Department and a Researcher with CIADA, UQU. His current research interests include evolutionary multiobjective optimization and machine learning techniques. He is currently involved in AI algorithms, focusing particularly on machine learning and optimization with a willingness to implement them in the context of decision making and solving combinatorial problems in real-world projects.